LLRF and beam loading cancellation

Fumihiko Tamura

J-PARC Ring RF group

June 2015

Overview

- introduction
  - magnetic alloy cavities of J-PARC RCS and MR
- low level rf system
- beam loading compensation
- experience of 1 MW-eq beam acceleration
- conclusion

Japan Proton Accelerator Research Complex

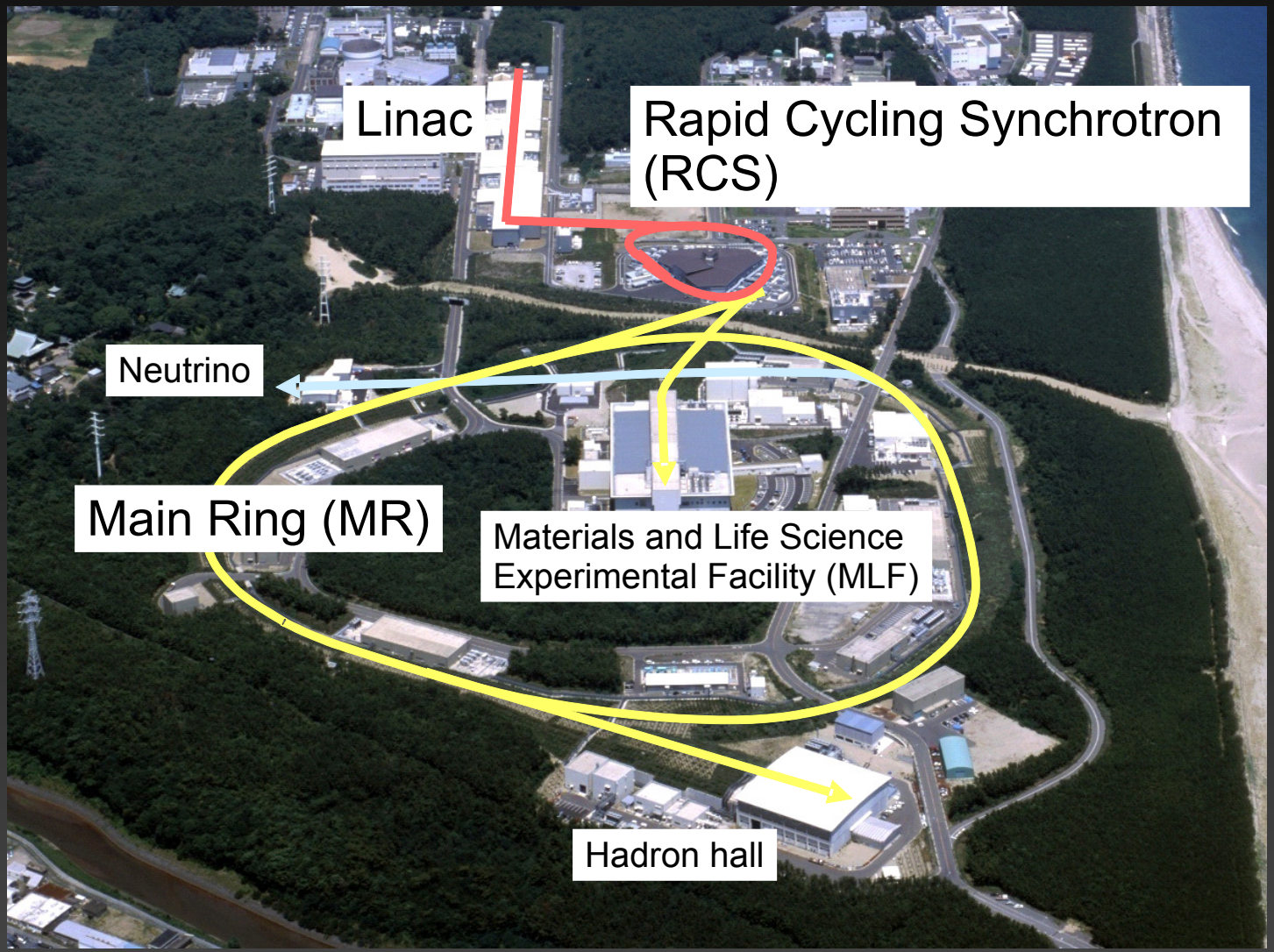

All rf cavities in RCS and MR are magnetic alloy (finemet) cavities.

Japan Proton Accelerator Research Complex

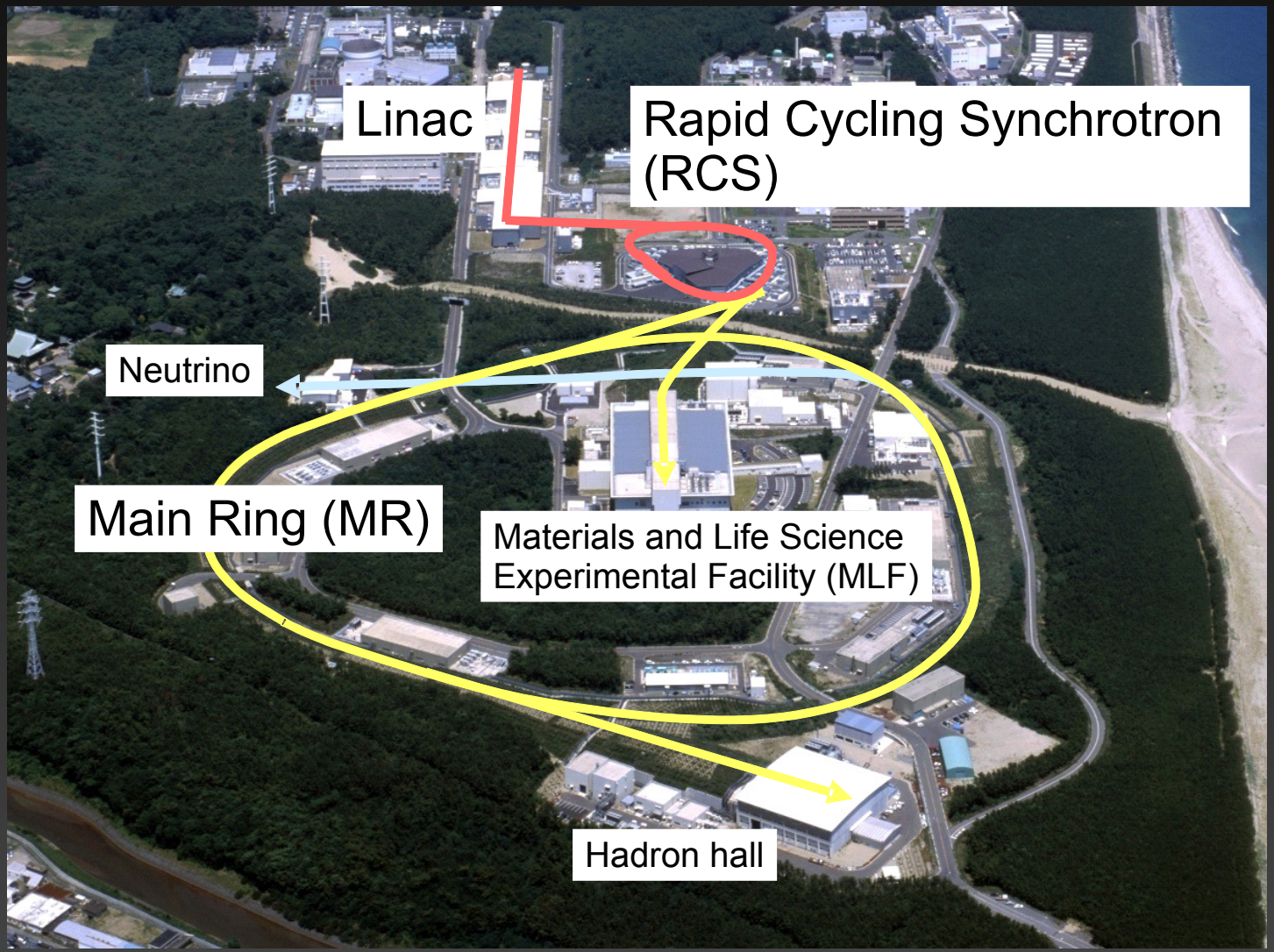

All rf cavities in RCS and MR are magnetic alloy (finemet) cavities.

J-PARC RCS/MR parameters

parameter	RCS	MR
circumference	348.333 m	1567.5 m
energy	(until 2013) 0.181–3 GeV (from 2014) 0.400–3 GeV	3–30 GeV
beam intensity	(design) 8.3×10^{13} ppp (achieved) 8.3×10^{13} ppp	(achieved) 1.8×10^{14} ppp
repetition freq/period	25 Hz	2.48 s
accelerating frequency	(until 2013) 0.938–1.671 MHz (from 2014) 1.227–1.671 MHz	1.671–1.721 MHz
harmonic number	2	9
maximum rf voltage	440 kV	280 kV
No. of cavities	12	8 (+1 for 2nd)
Q-value of rf cavity	2	22

High intensity:

- RCS: 1 MW-equivalent achieved, 500 kW user operation
- MR: 350 kW user operation for neutrino experiments

Magnetic Alloy (finemet)

Ring core formed by winding ribbon:

- large size core is possible
- RCS: 85 cm, MR: 80 cm

High gradient:

- constant shunt impedance
- high curie temperature
- lower μQf & R_p, heat must be removed by proper way, need strong rf amplifier chain

Wideband / low Q:

- can follow frequency sweep during acceleration without tuning bias loop, more simple LLRF
- dual harmonic operation is possible (RCS)
- wake voltage is multiharmonic $\rightarrow$ discussed in my latter part

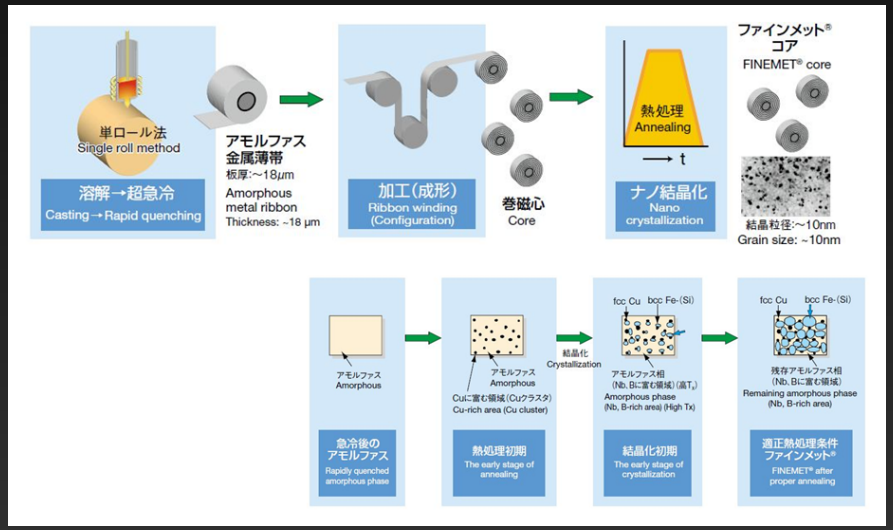

Production process of finemet cores.

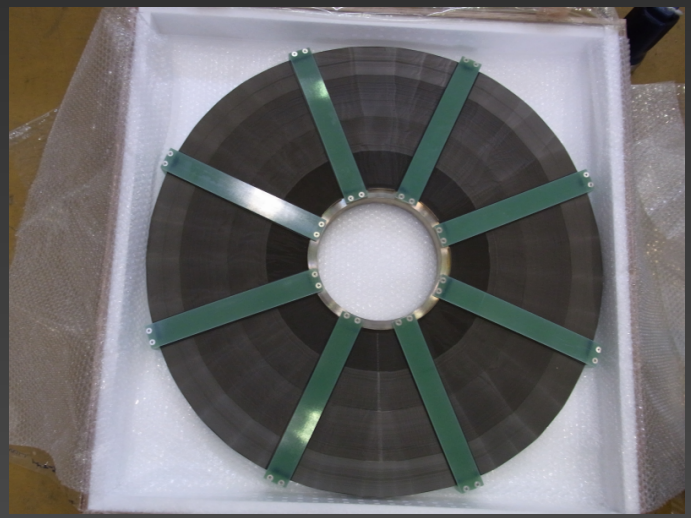

80 cm finemet cores for MR.

Magnetic Alloy (finemet)

Ring core formed by winding ribbon:

- large size core is possible
- RCS: 85 cm, MR: 80 cm

High gradient:

- constant shunt impedance
- high curie temperature
- lower μQf & R_p, heat must be removed by proper way, need strong rf amplifier chain

Wideband / low Q:

- can follow frequency sweep during acceleration without tuning bias loop, more simple LLRF
- dual harmonic operation is possible (RCS)
- wake voltage is multiharmonic $\rightarrow$ discussed in my latter part

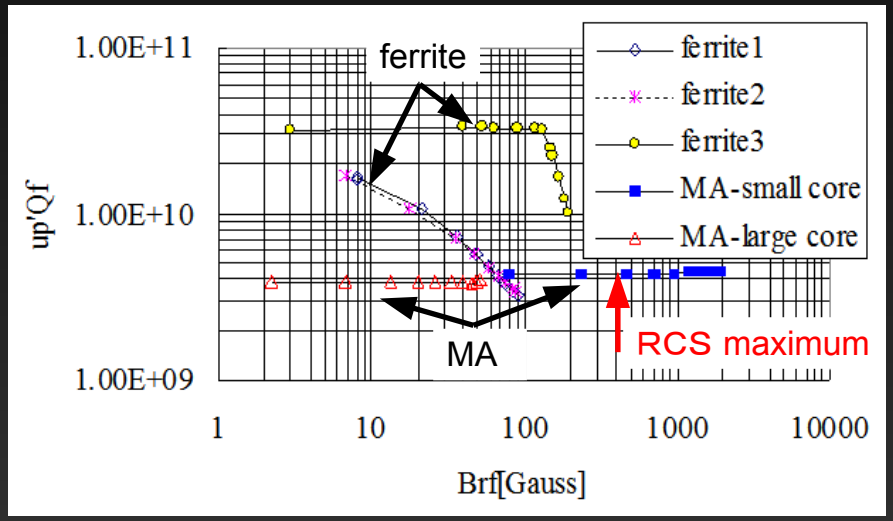

μQf dependency of B_{rf}

Magnetic Alloy (finemet)

Ring core formed by winding ribbon:

- large size core is possible
- RCS: 85 cm, MR: 80 cm

High gradient:

- constant shunt impedance
- high curie temperature
- lower μQf & R_p, heat must be removed by proper way, need strong rf amplifier chain

Wideband / low Q:

- can follow frequency sweep during acceleration without tuning bias loop, more simple LLRF
- dual harmonic operation is possible (RCS)
- wake voltage is multiharmonic
  $\rightarrow$ discussed in my latter part

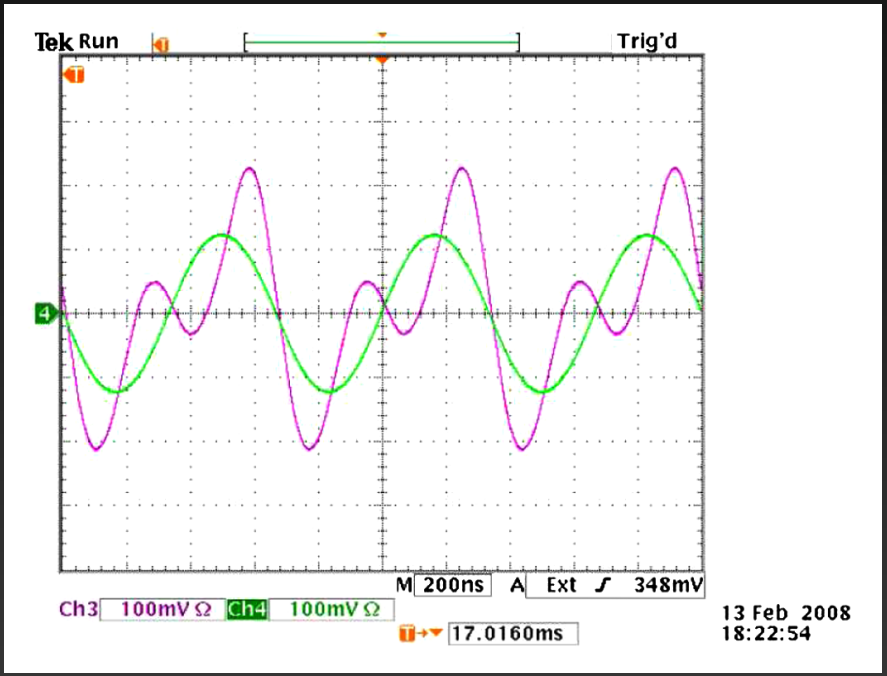

RCS cavity can be driven by dual harmonic.

Magnetic Alloy (finemet)

Ring core formed by winding ribbon:

- large size core is possible
- RCS: 85 cm, MR: 80 cm

High gradient:

- constant shunt impedance
- high curie temperature
- lower μQf & R_p, heat must be removed by proper way, need strong rf amplifier chain

Wideband / low Q:

- can follow frequency sweep during acceleration without tuning bias loop, more simple LLRF
- dual harmonic operation is possible (RCS)
- wake voltage is multiharmonic $\rightarrow$ discussed in my latter part

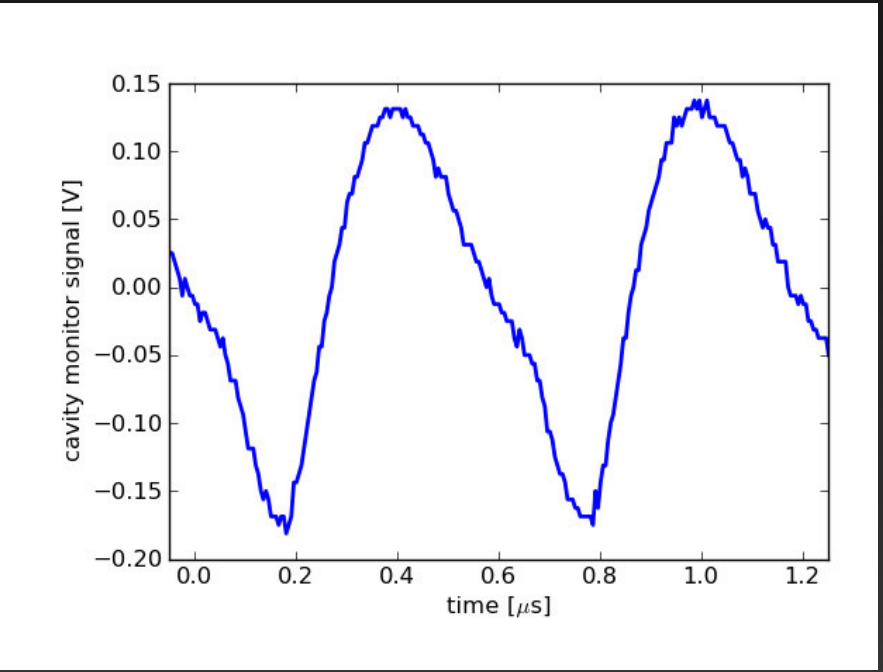

Typical wake voltage in RCS cavity.

RCS and MR cavities

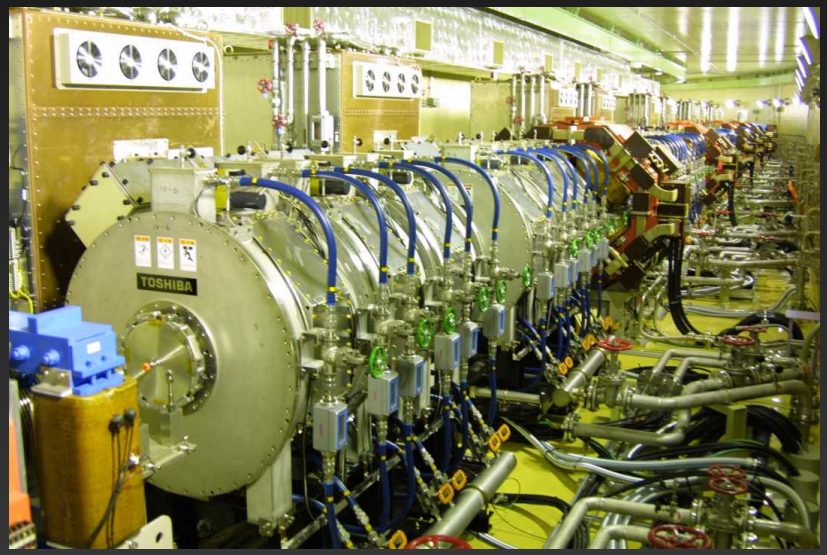

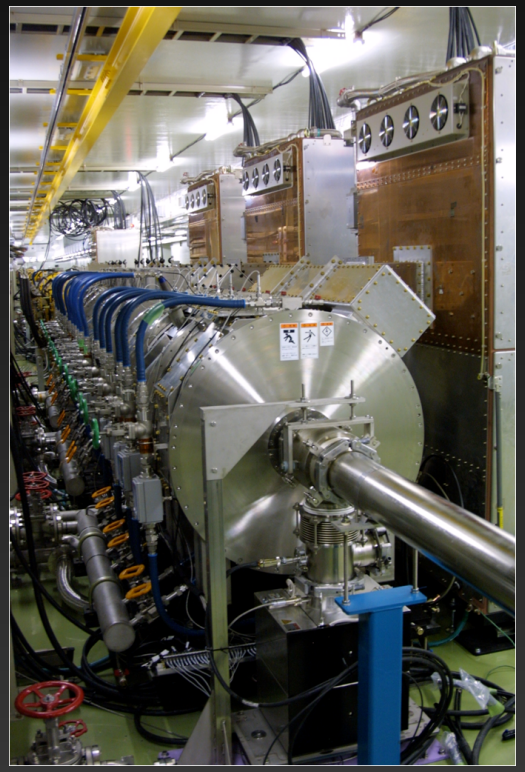

(Left) RCS cavities and (right) MR cavities

- 3-gaps / cavity, 18 cores / cavity
- $\sim$2 m long, maximum 40 kV / cavity
- strong rf power source: push-pull amplifier with TH558K, 10–12 kV, 92 A anode PS,

Further upgrade: new FT3L cavity

- Finemet FT3L, annealed with B-field has higher shunt impedance than FT3M
- We developed large size core annealing system using big magnet.

All existing 3-gap MR cavities will be replaced 4- and 5-gap FT3L cavity.

- existing amplifier chain and anode PS are used as is
- rf voltage 45 kV $\rightarrow$ 75 kV
- will generate 560 kV (present: 280 kV) for shorter cycle (2.48 s $\rightarrow$ 1 s)

First 5-gap cavity is successfully installed in the tunnel and operated.

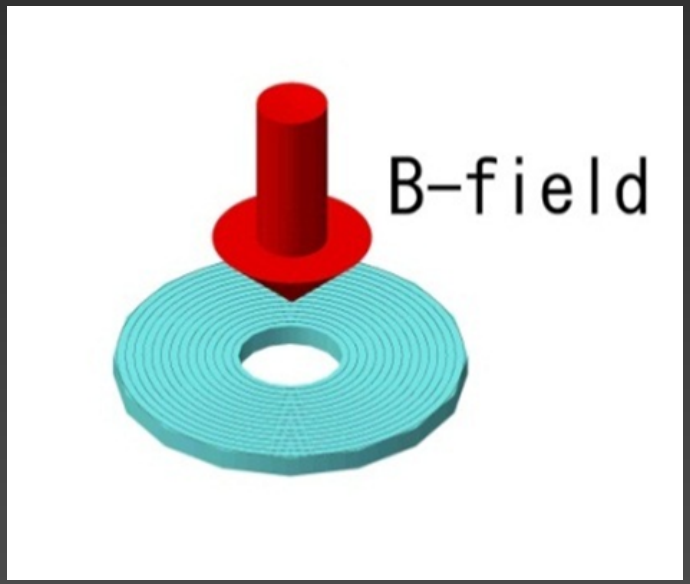

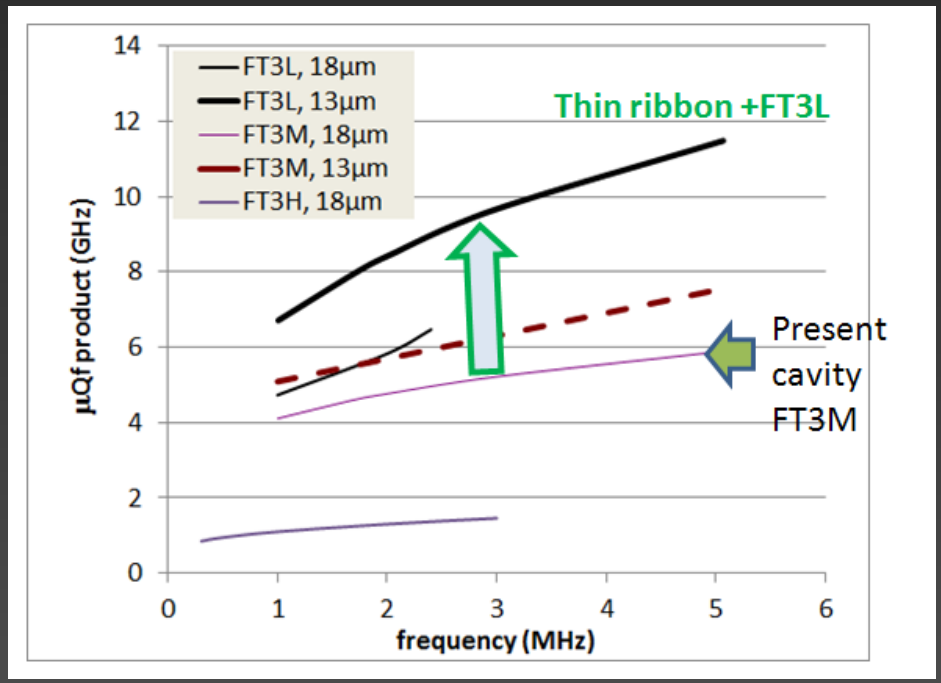

Further upgrade: new FT3L cavity

- Finemet FT3L, annealed with B-field has higher shunt impedance than FT3M
- We developed large size core annealing system using big magnet.

All existing 3-gap MR cavities will be replaced 4- and 5-gap FT3L cavity.

- existing amplifier chain and anode PS are used as is
- rf voltage 45 kV $\rightarrow$ 75 kV
- will generate 560 kV (present: 280 kV) for shorter cycle (2.48 s $\rightarrow$ 1 s)

First 5-gap cavity is successfully installed in the tunnel and operated.

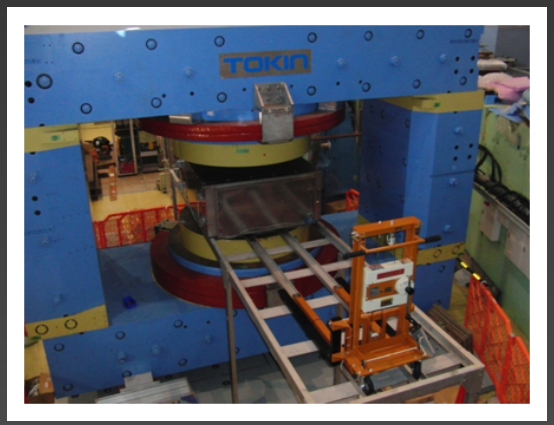

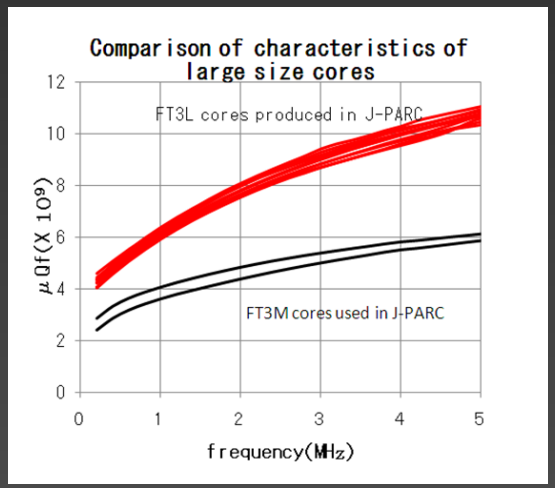

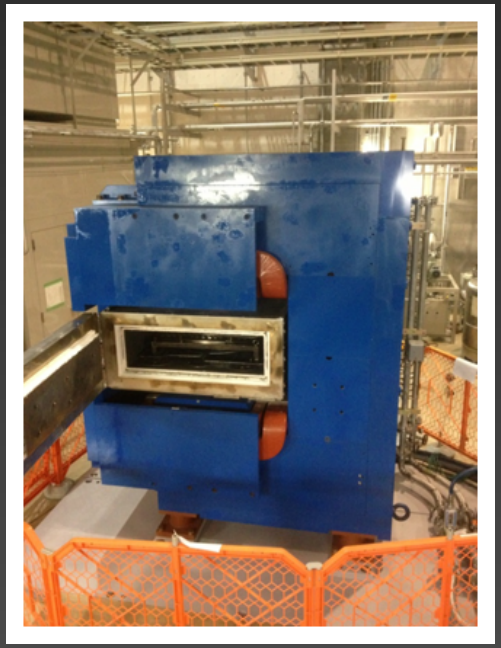

Further upgrade: new FT3L cavity

- Finemet FT3L, annealed with B-field has higher shunt impedance than FT3M
- We developed large size core annealing system using big magnet.

All existing 3-gap MR cavities will be replaced 4- and 5-gap FT3L cavity.

- existing amplifier chain and anode PS are used as is
- rf voltage 45 kV $\rightarrow$ 75 kV
- will generate 560 kV (present: 280 kV) for shorter cycle (2.48 s $\rightarrow$ 1 s)

First 5-gap cavity is successfully installed in the tunnel and operated.

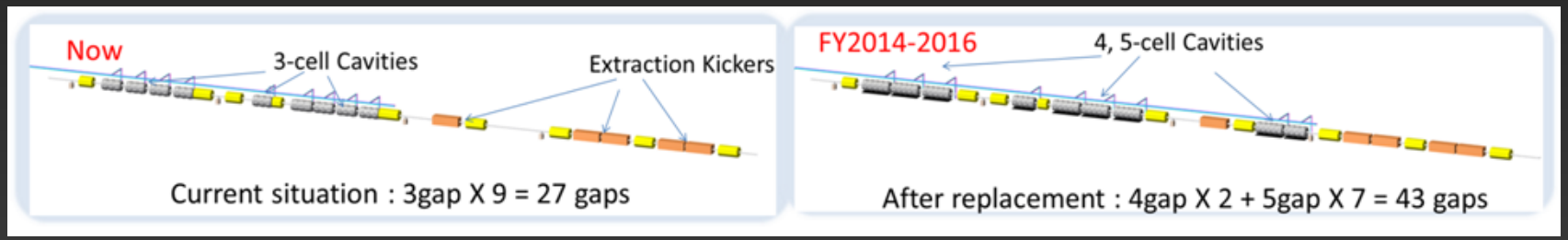

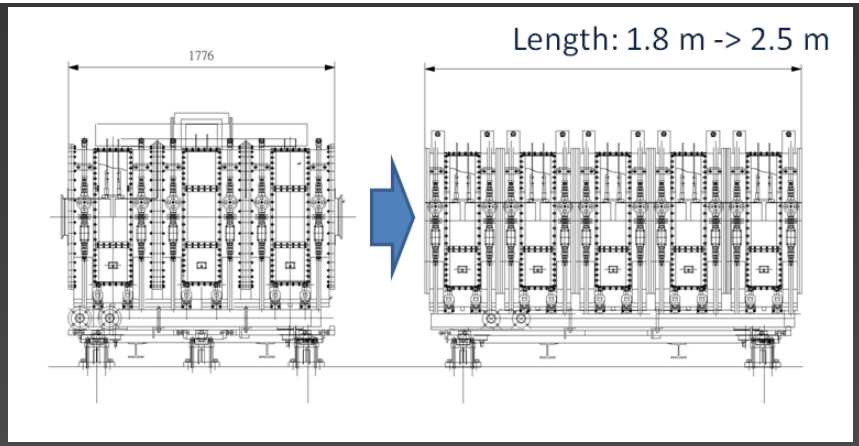

Cavity replacement scenario and 3 and 5-gap cavity.

Further upgrade: new FT3L cavity

- Finemet FT3L, annealed with B-field has higher shunt impedance than FT3M
- We developed large size core annealing system using big magnet.

All existing 3-gap MR cavities will be replaced 4- and 5-gap FT3L cavity.

- existing amplifier chain and anode PS are used as is
- rf voltage 45 kV $\rightarrow$ 75 kV
- will generate 560 kV (present: 280 kV) for shorter cycle (2.48 s $\rightarrow$ 1 s)

First 5-gap cavity is successfully installed in the tunnel and operated.

5-gap FT3L cavity in Hendel test bench.

Low level rf control systems

J-PARC LLRF control system overview

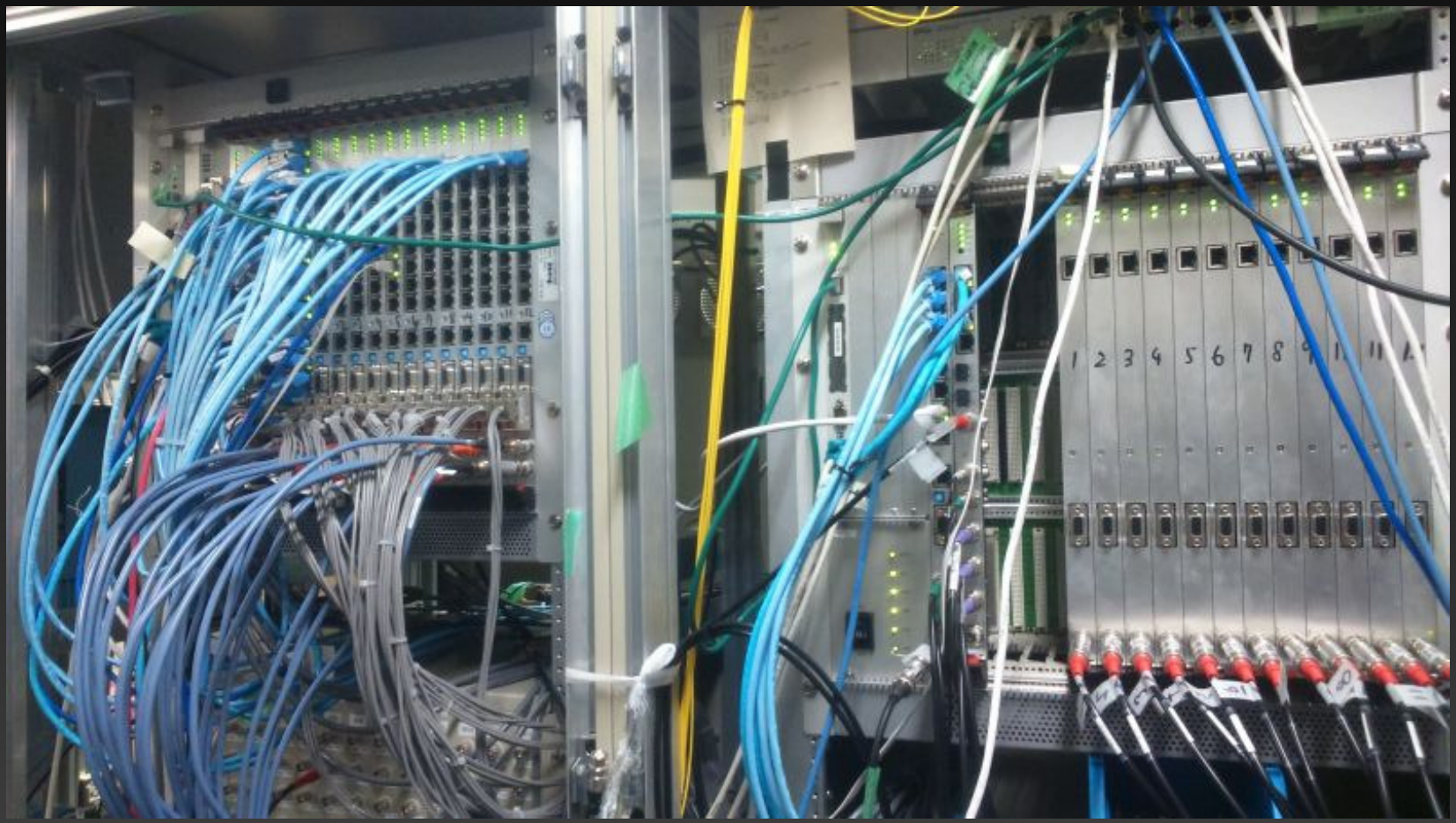

RCS LLRF control system.

- developed JFY 2003–2006
- VME based, 9U height
- designed to handle multiharmonic signals
- FPGA based, no DSPs

J-PARC LLRF control system overview

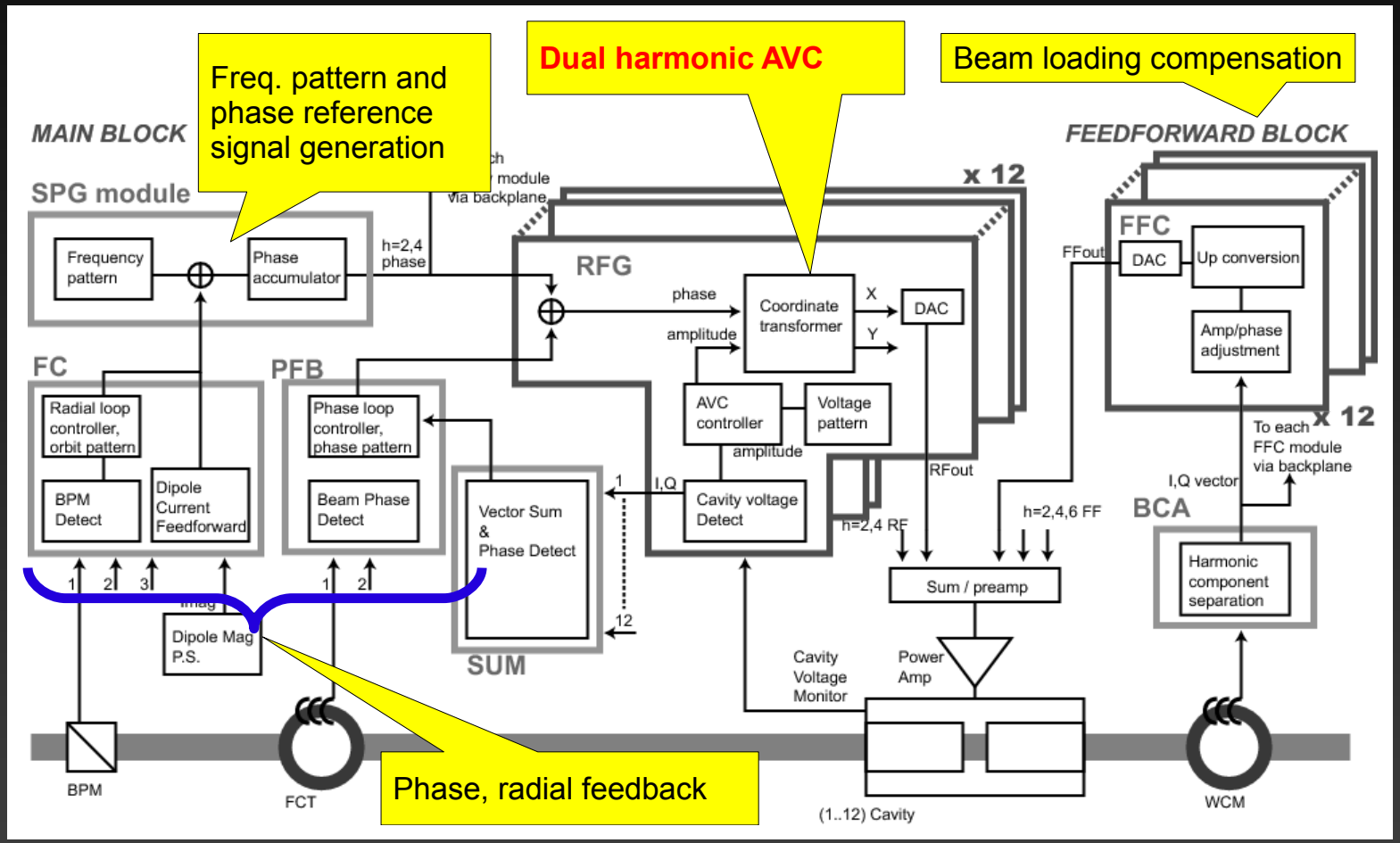

Block diagram of RCS LLRF control system (MR is similar).

- developed JFY 2003–2006
- VME based, 9U height
- designed to handle multiharmonic signals
- FPGA based, no DSPs

J-PARC LLRF control system overview

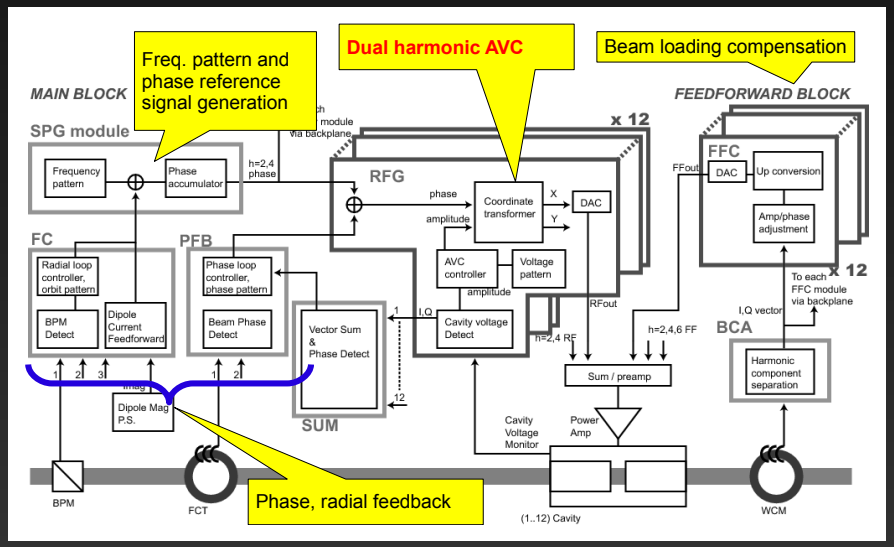

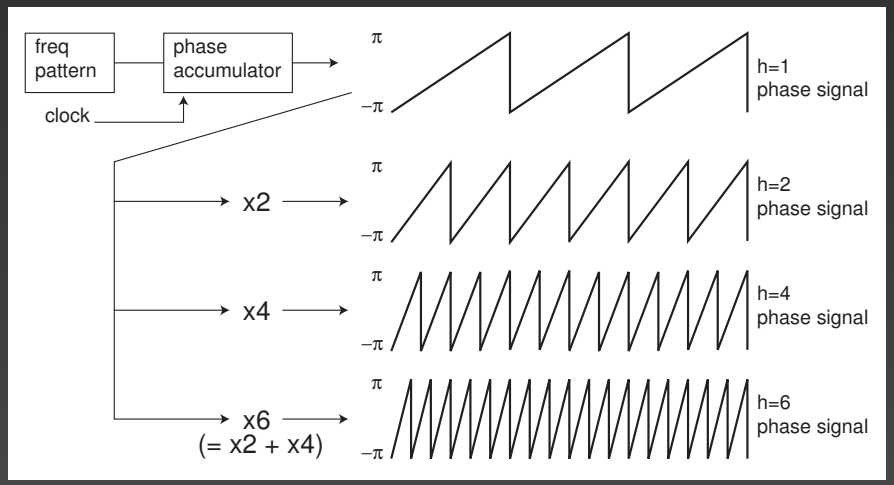

LLRF functions:

- fixed system clock (36 MHz)
- DDS (direct digital synthesis)-based multi-harmonic RF generation for cavity drive and signal detection
- common feedbacks for stabilizing the beam
  - AVC, cavity voltage control
  - phase FB (RF phase)
  - radial FB (frequency)
- rf feedforward system for compensating the heavy beam loading
- misc. functions; synchronization, chopper timing

Dual harmonic AVC

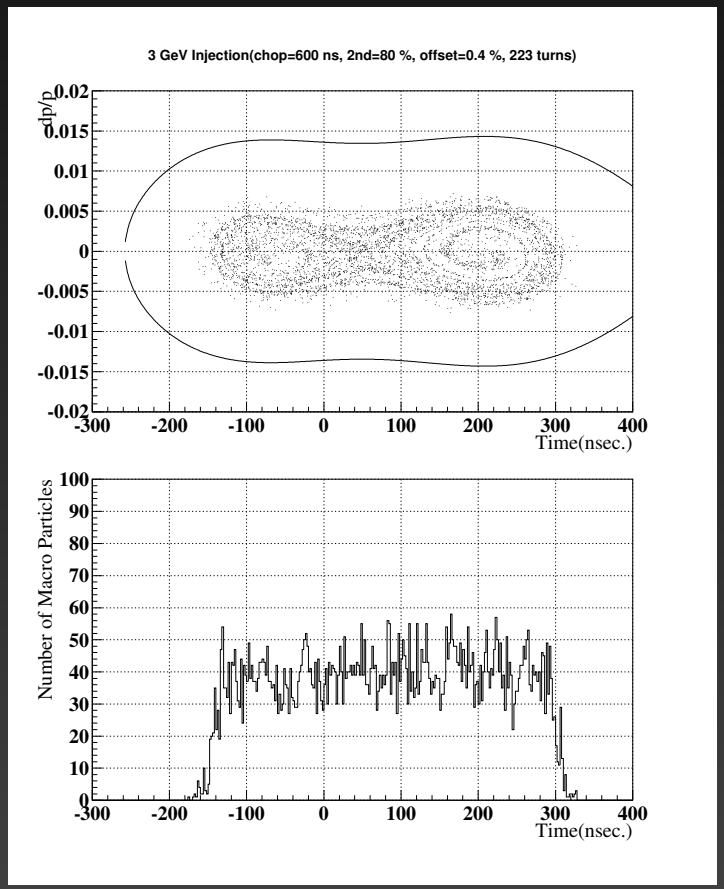

RCS: wide-band cavity, $Q = 2$

- No tuning loop
- A single cavity is driven by the superposition of multi-harmonic RF signals
  - the fundamental RF ($h = 2$): for acceleration of the beam
  - the second harmonic RF ($h = 4$): for the bunch shape control by modifying the RF bucket. Increasing the bunching factor to alleviate the space charge effects

Precise control of the harmonic voltages is necessary.

Dual harmonic AVC

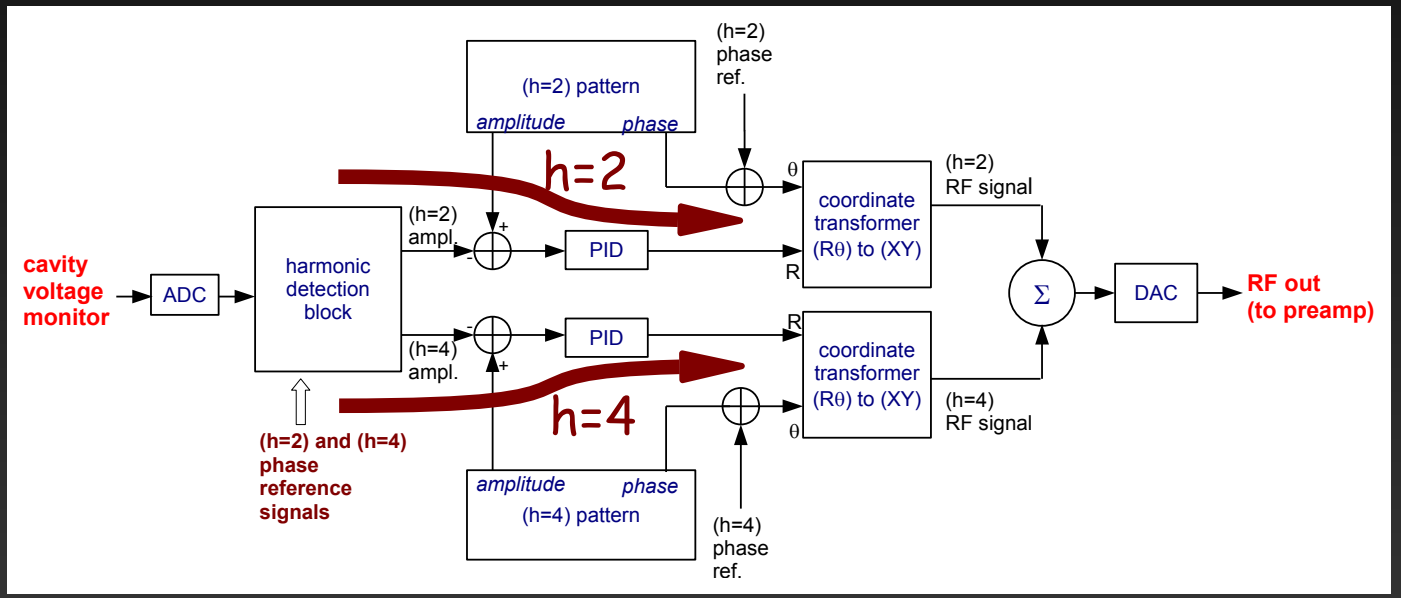

- frequency is low (several MHz): cavity voltage is directly converted into digital by ADC (36 Ms/s)
- harmonic detection blocks
  - amplitudes of $(h = 2)$ and $(h = 4)$ are detected
- compared with the amplitude patterns
- PID (Proportional-Integral-Derivative) controllers
- coordinate transformer, (R, θ) to (X, Y)
  - RF signal is generated, using phase pattern
- $(h = 2)$ and $(h = 4)$ RF signals are summed; dual-harmonic RF signals
- DAC

Dual harmonic AVC

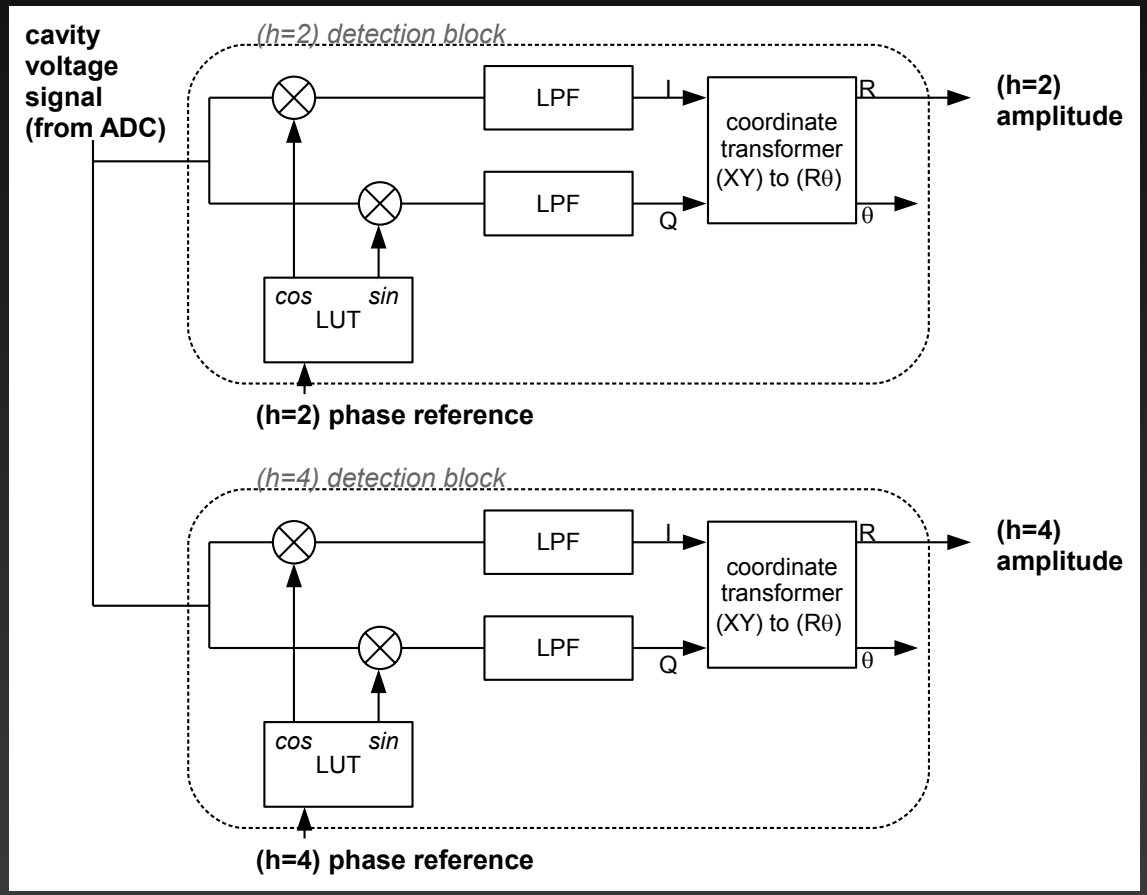

Harmonic detection block.

- I/Q demodulation technique is used
- the LPF must reject the nearest harmonics: $(h = 1)$ and $(h = 3)$. Minimum separation is at injection, 0.47 MHz
- I/Q vector: $I_{(2,4)} = A_{(2,4)} \sin(\phi_{(2,4)})$, $Q_{(2,4)} = A_{(2,4)} \cos(\phi_{(2,4)})$
- Coordinate transformer, (X, Y) to (R, θ)

Dual harmonic AVC

- the amplitudes of the fundamental and the second harmonic are detected and compared with the patterns
- the amplitude of each harmonic is controlled independently
- dual-harmonic AVC is working very well

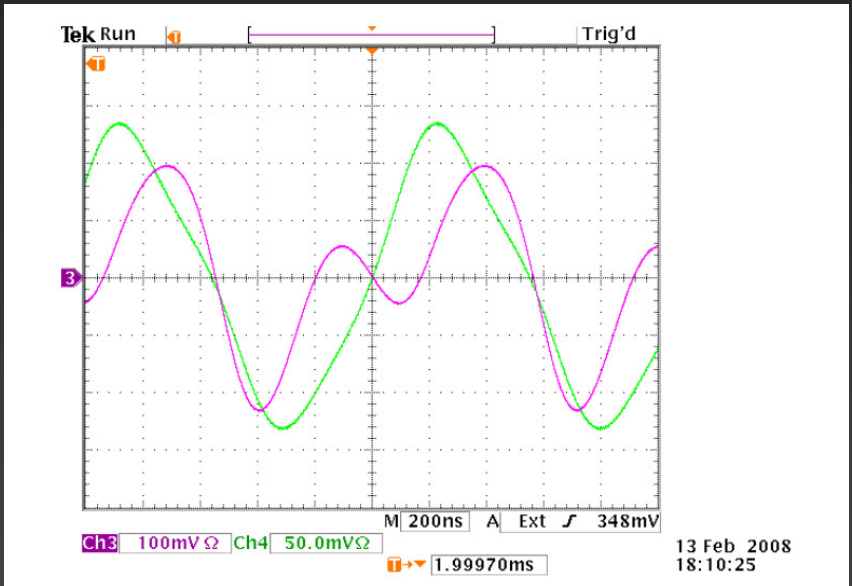

Cavity voltage monitor signal. Green: fundamental only, Pink: with 80% second harmonic.

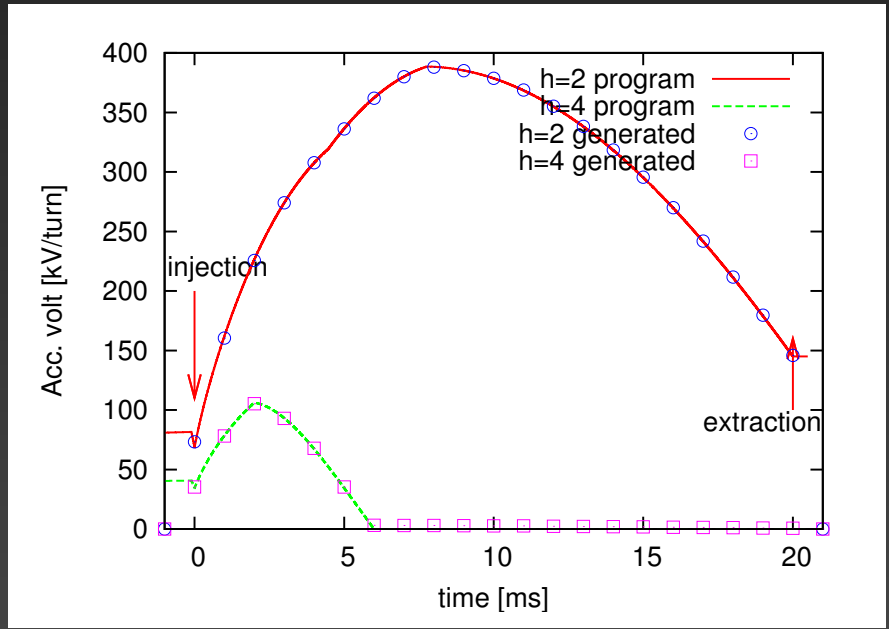

Comparison of the program and measurement.

Phase feedback

Roles of phase feedback:

- suppress longitudinal dipole oscillation (accelerating harmonic, $h = 2$)
- lock second harmonic ($h = 4$) rf phase to fundamental rf

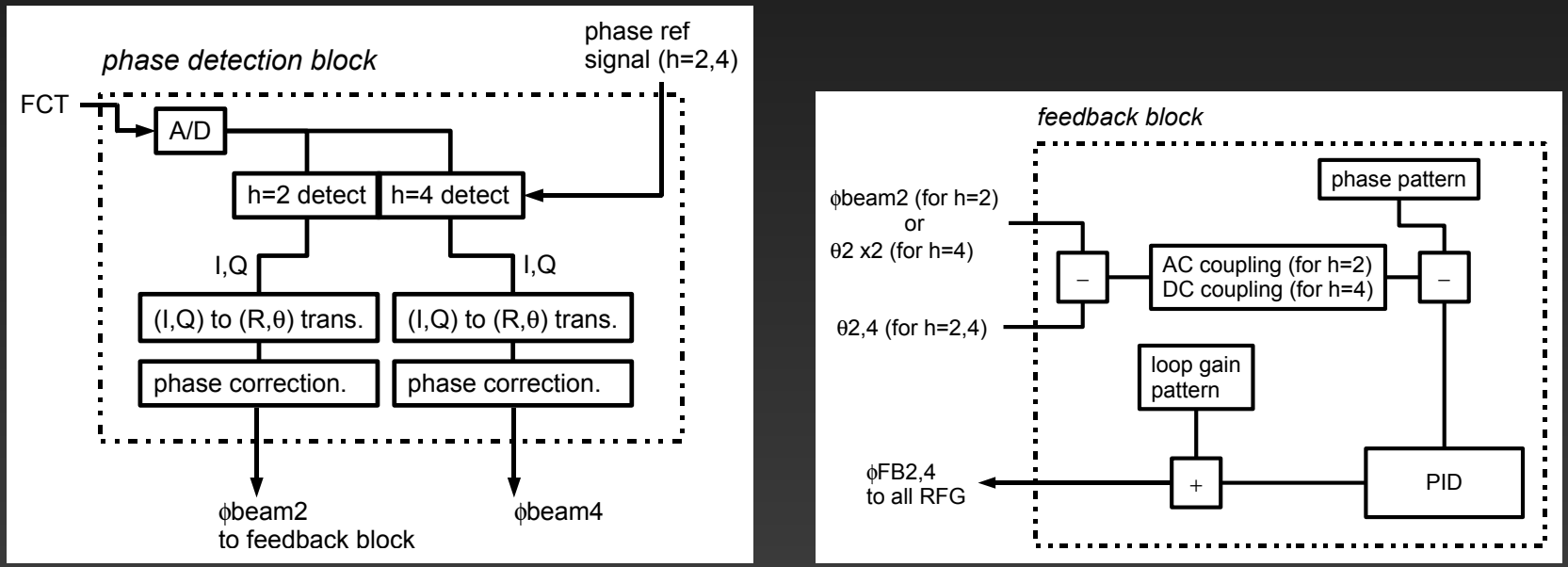

Block diagram of phase feedback.

- phase modulation used (not frequency modulation). For second harmonic, it is natural
- good for phase control of extracted beams (discussed later)

Phase feedback

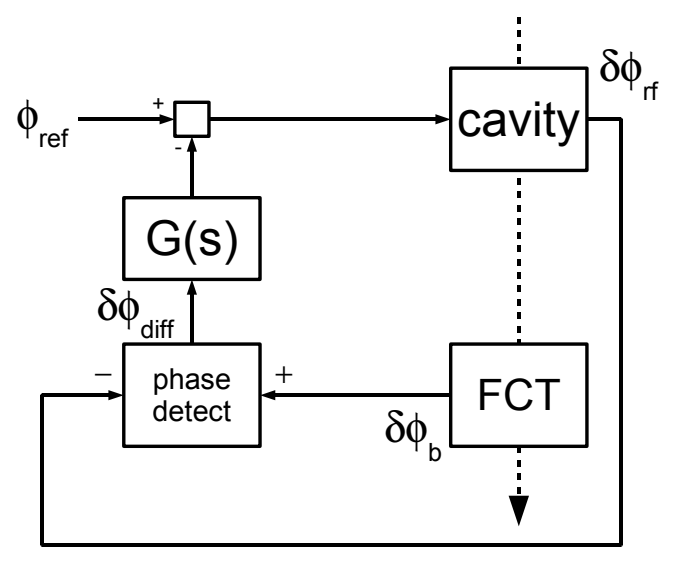

Block diagram of phase feedback.

$G(s) = K_P + \frac{K_I}{s}$ (K_P, K_I are proportional and integrator gain), the transfer function with feedback is:

$$\frac{\delta\phi_{\mathrm{diff}}(s)}{\delta\phi_{\mathrm{rf}}(s)} = \frac{B'(s)}{1 + B'(s)G(s)} = \frac{s^2}{(K_P - 1)s^2 + K_I s - \omega_s^2}$$

- if $K_I = 0$, the pole $s = \pm\sqrt{\frac{\omega_s^2}{K_P - 1}}$ is real or pure imaginary, not stable
- transfer function with only integration gain:

$$\frac{\delta\phi_{\mathrm{diff}}(s)}{\delta\phi_{\mathrm{rf}}(s)} = \frac{-s^2}{s^2 - K_I s + \omega_s^2}$$

if $K_I < 0$, the real part of the pole becomes negative and the oscillation damped

Phase feedback

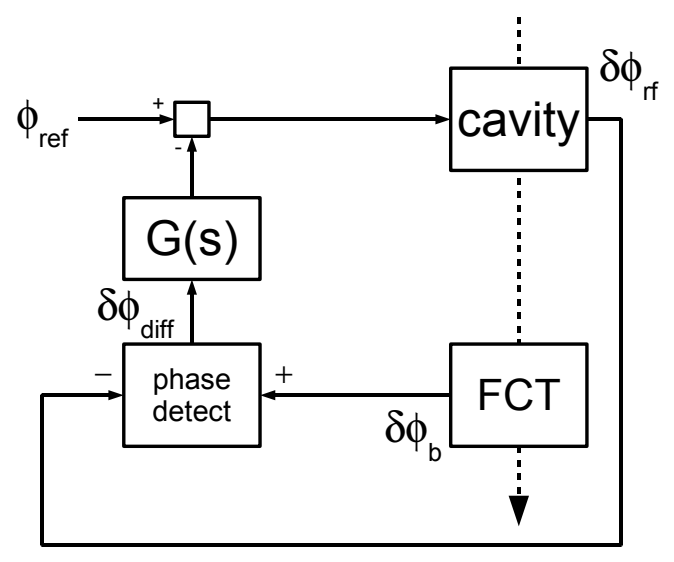

Block diagram of phase feedback.

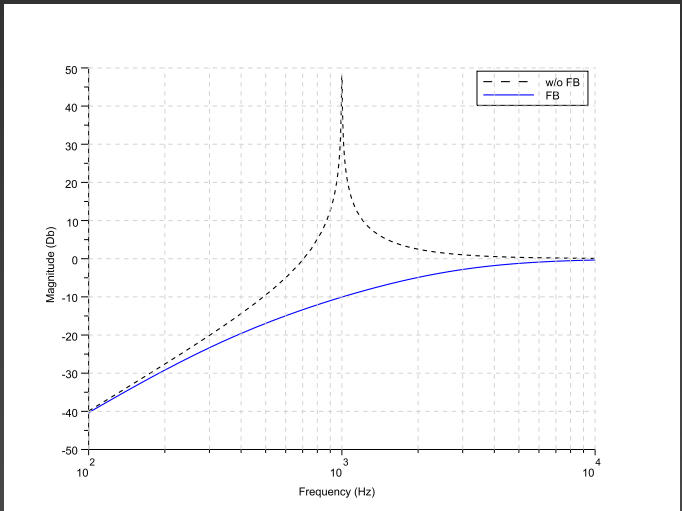

Bode plots without and with phase feedback ($f_s = 1000$ Hz).

$G(s) = K_P + \frac{K_I}{s}$ (K_P, K_I are proportional and integrator gain), the transfer function with feedback is:

$$\frac{\delta\phi_{\text{diff}}(s)}{\delta\phi_{\text{rf}}(s)} = \frac{B'(s)}{1 + B'(s)G(s)} = \frac{s^2}{(K_P - 1)s^2 + K_I s - \omega_s^2}$$

- if $K_I = 0$, the pole $s = \pm\sqrt{\frac{\omega_s^2}{K_P - 1}}$ is real or pure imaginary, not stable
- transfer function with only integration gain:

$$\frac{\delta\phi_{\text{diff}}(s)}{\delta\phi_{\text{rf}}(s)} = \frac{-s^2}{s^2 - K_I s + \omega_s^2}$$

if $K_I < 0$, the real part of the pole becomes negative and the oscillation damped

Damping of dipole oscillation

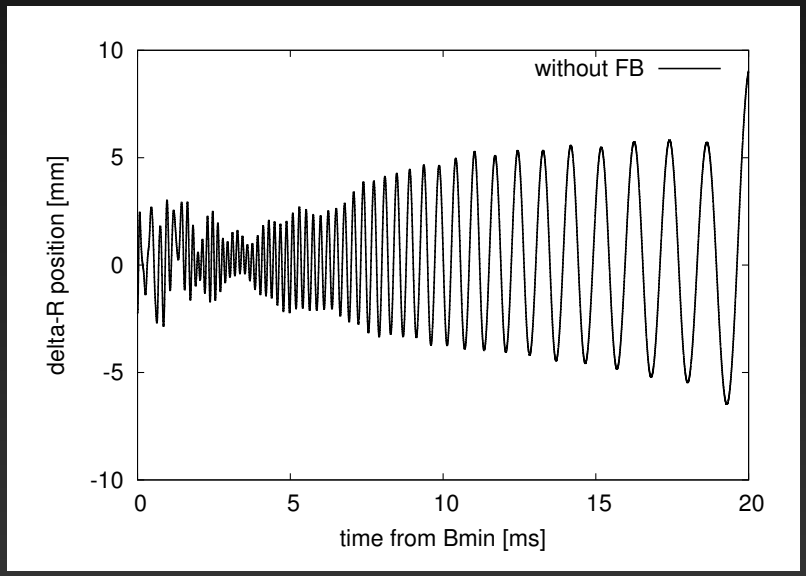

Comparison of radial excursions.

- without phase feedback, dipole oscillation continues till end of acceleration
- by phase feedback of accelerating harmonic ($h = 2$), the oscillation is damped successfully

Damping of dipole oscillation

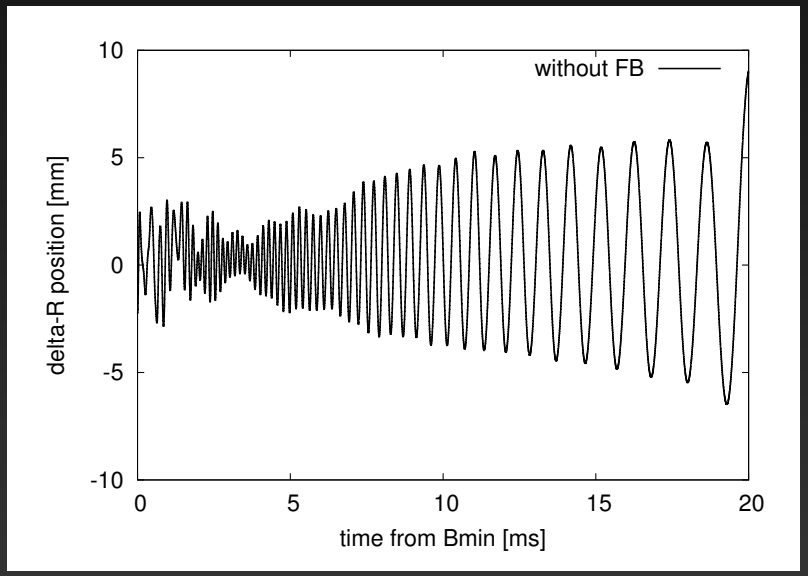

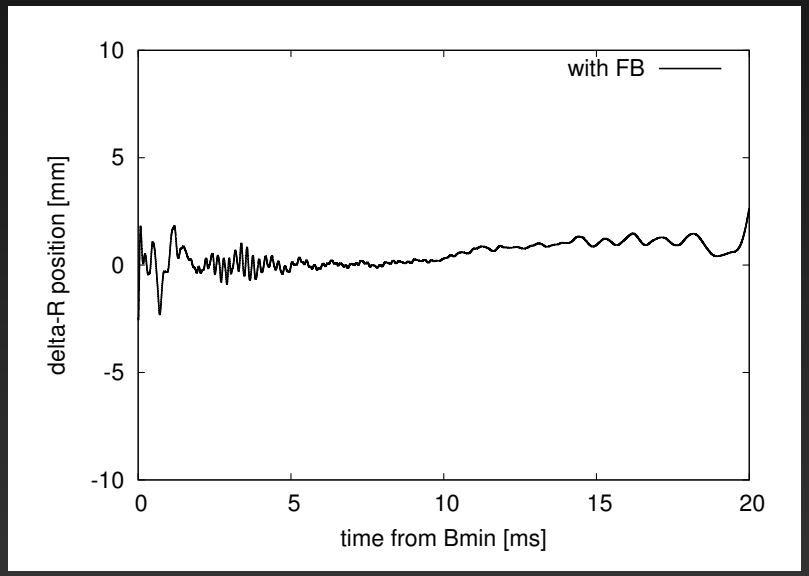

Comparison of radial excursions.

- without phase feedback, dipole oscillation continues till end of acceleration
- by phase feedback of accelerating harmonic ($h = 2$), the oscillation is damped successfully

Second harmonic phase sweep

- The second harmonic phase is swept so that the RF bucket shape is modified during the injection period
- Efficient way to distribute the particles

$$\phi_{(h=4)} = \frac{\phi_{\mathrm{sweep}}}{T_{\mathrm{inj}}} \left(t - \frac{T_{\mathrm{inj}}}{2} \right) - 2\phi_s \ [\mathrm{deg}]$$

$\phi_{(h=4)}$: the second harmonic phase
ϕ_{sweep}: the sweep range that was set to 80 deg
T_{inj}: the duration of the injection
ϕ_s: the synchronous phase

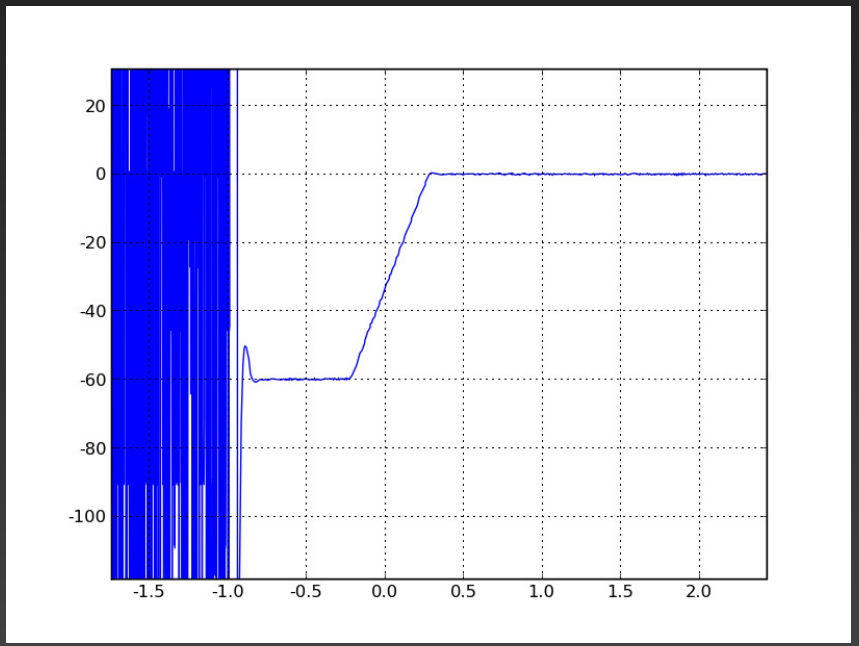

Second harmonic phase sweep example. horizontal-axis: time [ms], vertical axis: relative phase of the second harmonic to the fundamental minus ϕ_s.

Achievement of longitudinal injection painting

Using the LLRF functions, longitudinal injection painting during RCS injection period is achieved:

- momentum offset -0.2%(by frequency offset)
- large amplitude ($\sim$80% of fundamental) second harmonic rf
- second harmonic phase sweep, 100 degrees

Achievement of longitudinal injection painting

Without (left) and with (right) longitudinal painting

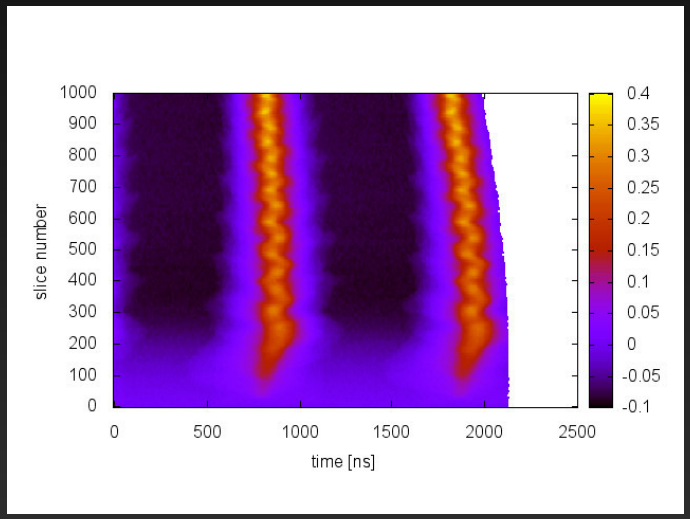

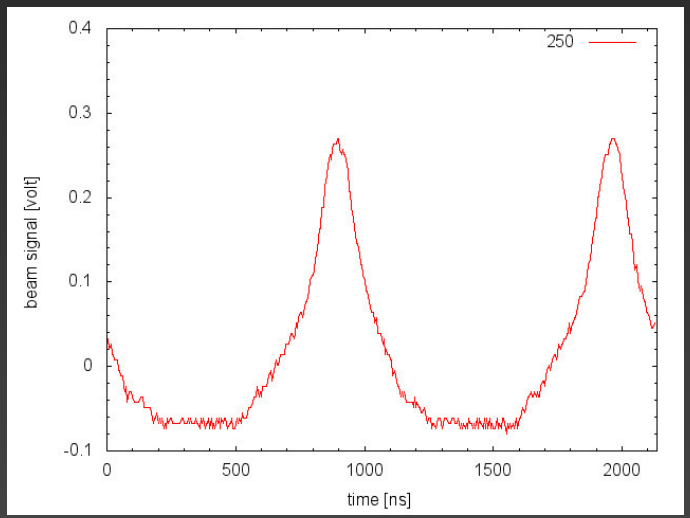

- flat bunch generated by longitudinal painting

Achievement of longitudinal injection painting

Without (left) and with (right) longitudinal painting

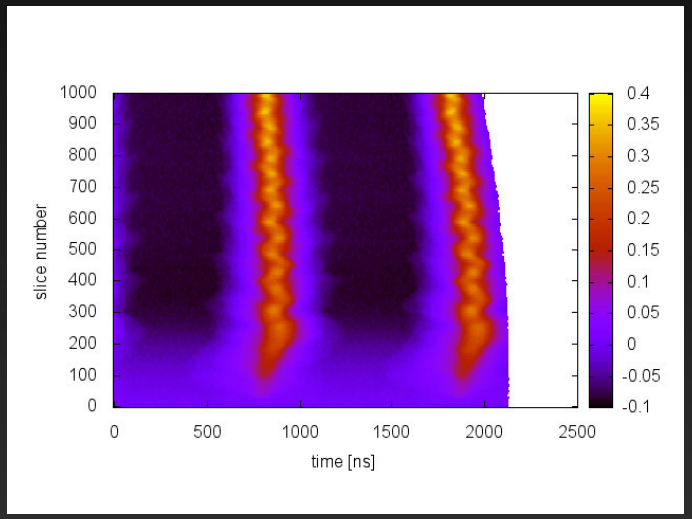

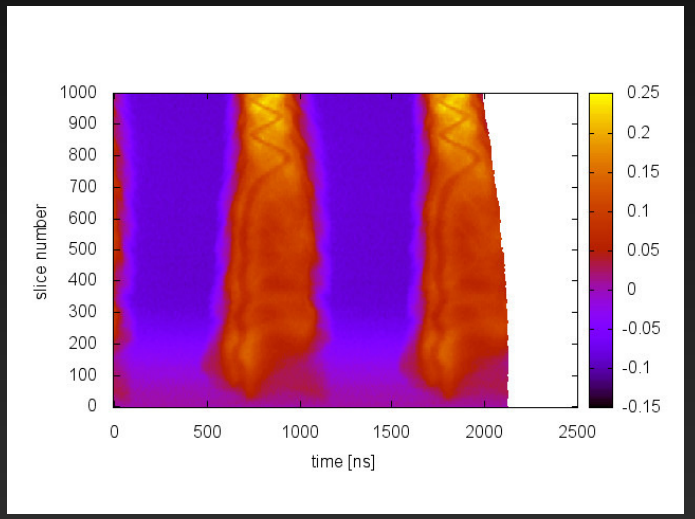

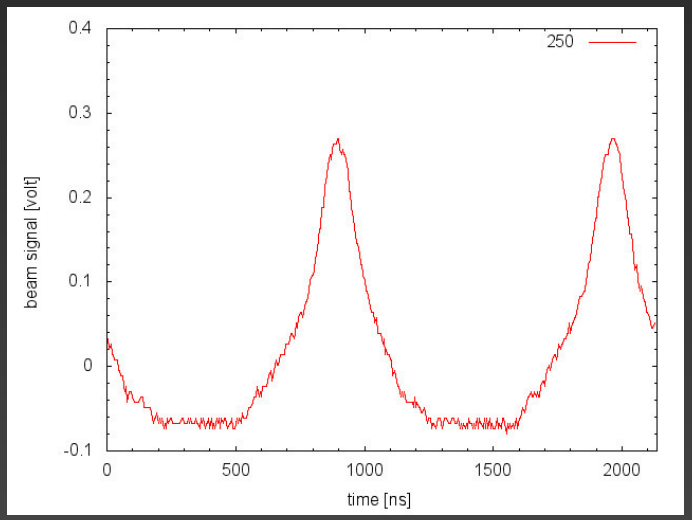

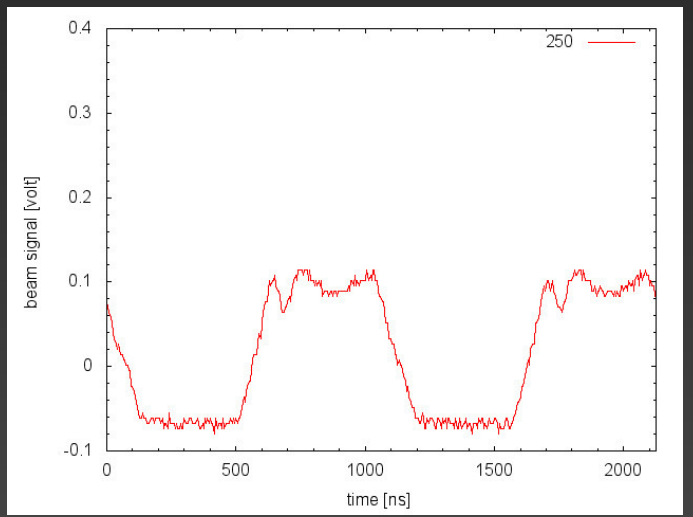

- flat bunch generated by longitudinal painting

Achievement of longitudinal injection painting

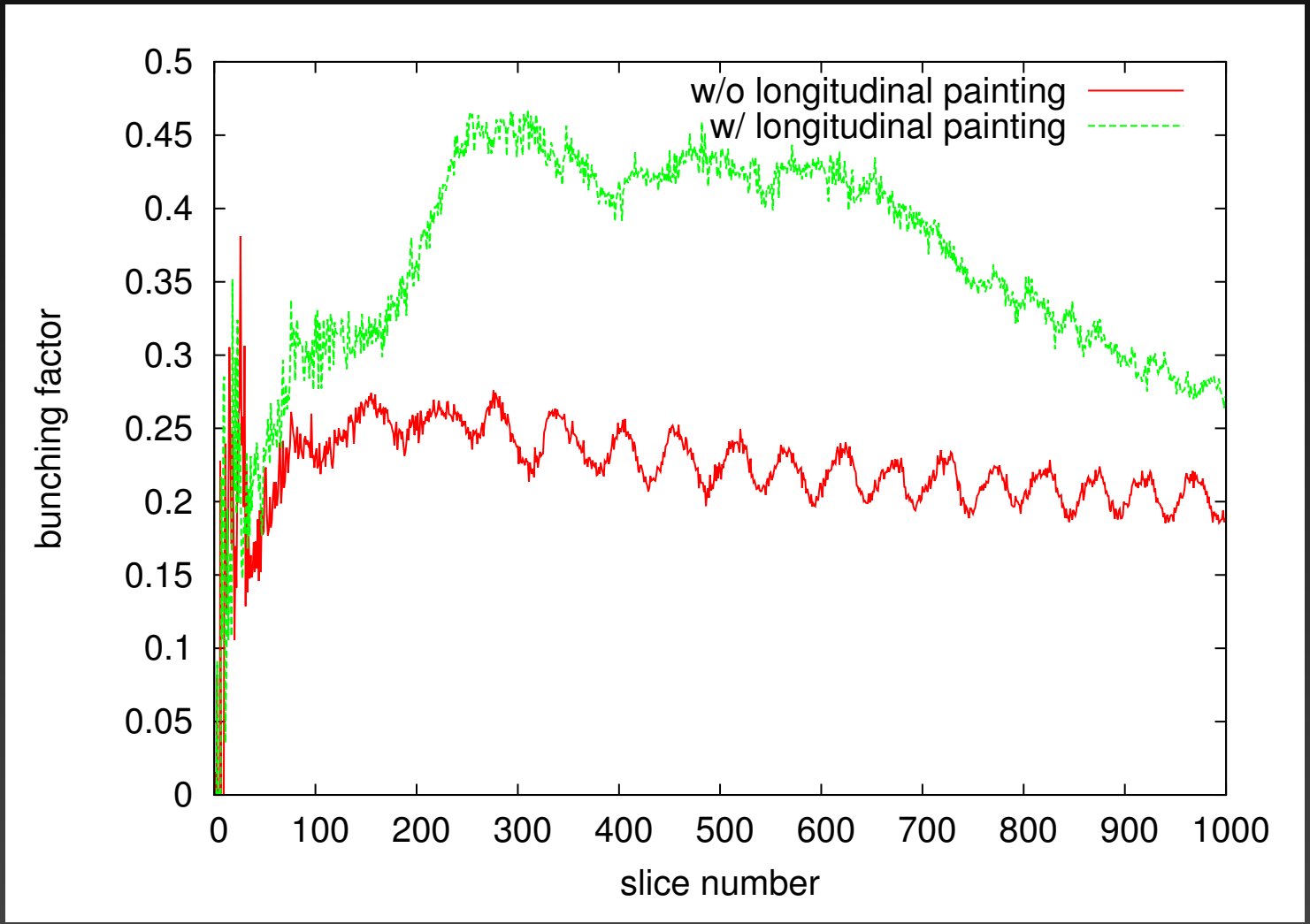

Bunching factor improved, 0.25 $\rightarrow$ 0.45.

Frequency correction without radial feedback

- B-field is stable after the warming-up
- frequency is reproducible thanks to DDS
- we adjust the accelerating frequency pattern without radial loop
- we take an orbit signal of a full accelerating cycle and correct the frequency pattern:

$$\Delta f_{\text{correction}} = f_{\text{rf}} \times \eta \times \frac{dp}{p}$$

  dp/p is obtained using a set of BPM at high dispersion
- orbit correction working well with a few iterations
- dp/p is stable after correction

Frequency correction without radial feedback

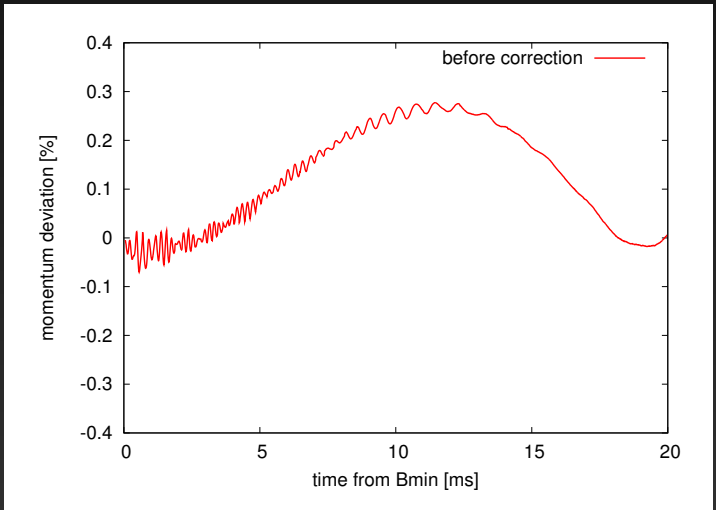

dp/p with initial frequency pattern, assumed that B-field is sinusoidal.

- B-field is stable after the warming-up
- frequency is reproducible thanks to DDS
- we adjust the accelerating frequency pattern without radial loop
- we take an orbit signal of a full accelerating cycle and correct the frequency pattern:

$$\Delta f_{\text{correction}} = f_{\text{rf}} \times \eta \times \frac{dp}{p}$$

  dp/p is obtained using a set of BPM at high dispersion
- orbit correction working well with a few iterations
- dp/p is stable after correction

Frequency correction without radial feedback

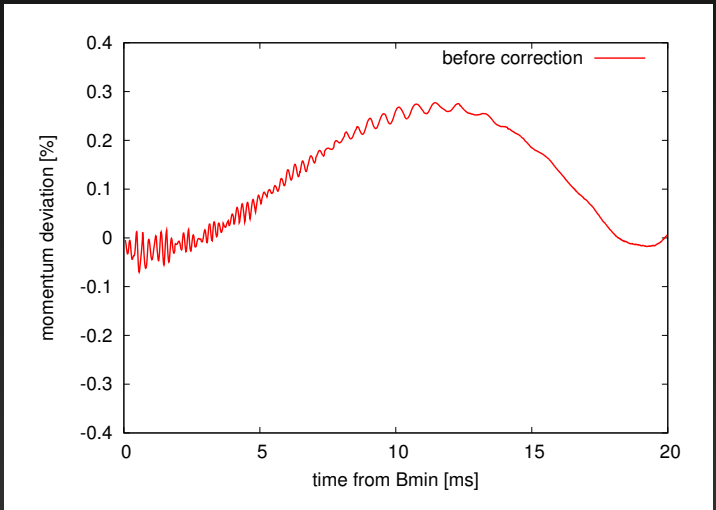

dp/p with initial frequency pattern, assumed that B-field is sinusoidal.

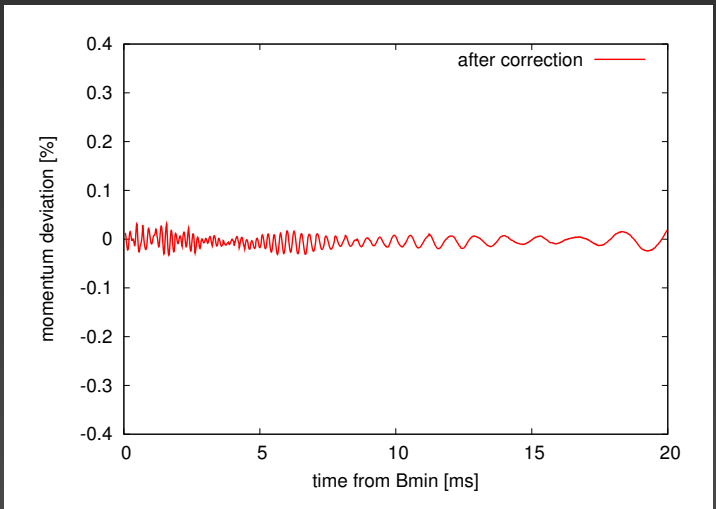

dp/p after frequency correction.

- B-field is stable after the warming-up
- frequency is reproducible thanks to DDS
- we adjust the accelerating frequency pattern without radial loop
- we take an orbit signal of a full accelerating cycle and correct the frequency pattern:

$$\Delta f_{\mathrm{correction}} = f_{\mathrm{rf}} \times \eta \times \frac{dp}{p}$$

  dp/p is obtained using a set of BPM at high dispersion
- orbit correction working well with a few iterations
- dp/p is stable after correction

Synchronization

Synchronization to the neutron chopper and MR rf bucket is important.

Very small tolerance of beam timing jitter:

- MLF: for neutron chopper: $\pm$100 ns
- MR: several degrees of rf phase: $\pm$10ns

Synchronization

Our solution: neutron chopper and beam are synchronized to fixed 25 Hz timing.

- timing system based on precise master clock by synthesizer, not synchronized to the AC power line
  → eliminate effects due to variation of AC line frequency (0.1 Hz maximum)
- DDS (direct digital synthesis) based rf signal generation
  → reproducible rf signal / phase generation
- no radial feedback, which modulates rf frequency

For low intensity beams, the solution above is enough.
→ issues for high intensity beams.

Synchronization

Our solution: neutron chopper and beam are synchronized to fixed 25 Hz timing.

- timing system based on precise master clock by synthesizer, not synchronized to the AC power line
  → eliminate effects due to variation of AC line frequency (0.1 Hz maximum)
- DDS (direct digital synthesis) based rf signal generation
  → reproducible rf signal / phase generation
- no radial feedback, which modulates rf frequency

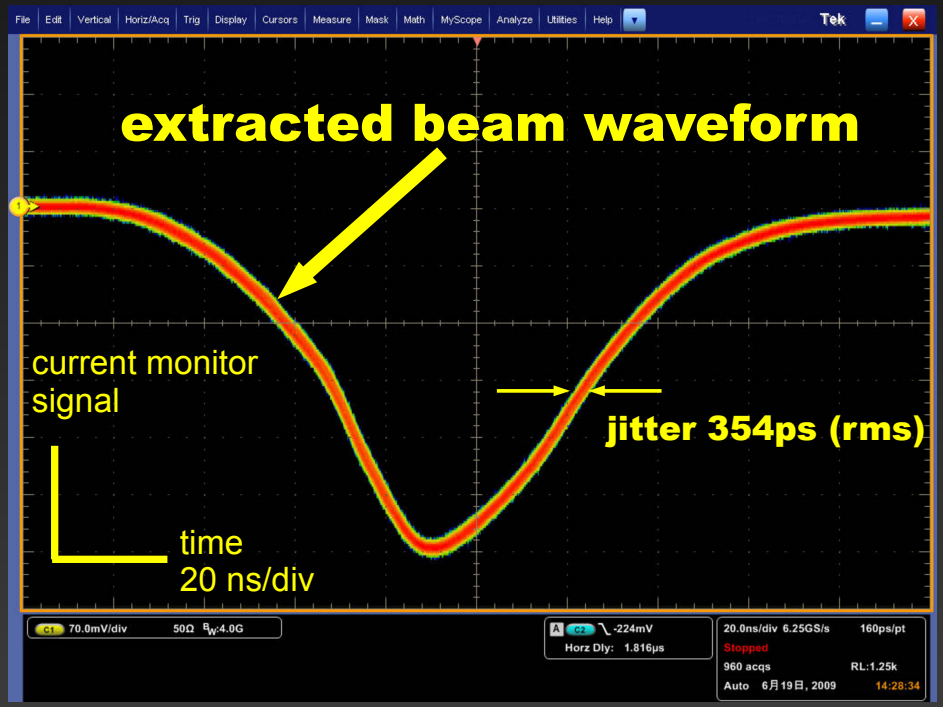

18 kW beam, superposition of $\sim$ 1000 beam waveforms at the extraction beam line. Very low timing jitter of 354 ps (RMS) was achieved.

For low intensity beams, the solution above is enough.
→ issues for high intensity beams.

Synchronization

Our solution: neutron chopper and beam are synchronized to fixed 25 Hz timing.

- timing system based on precise master clock by synthesizer, not synchronized to the AC power line
  → eliminate effects due to variation of AC line frequency (0.1 Hz maximum)
- DDS (direct digital synthesis) based rf signal generation
  → reproducible rf signal / phase generation
- no radial feedback, which modulates rf frequency

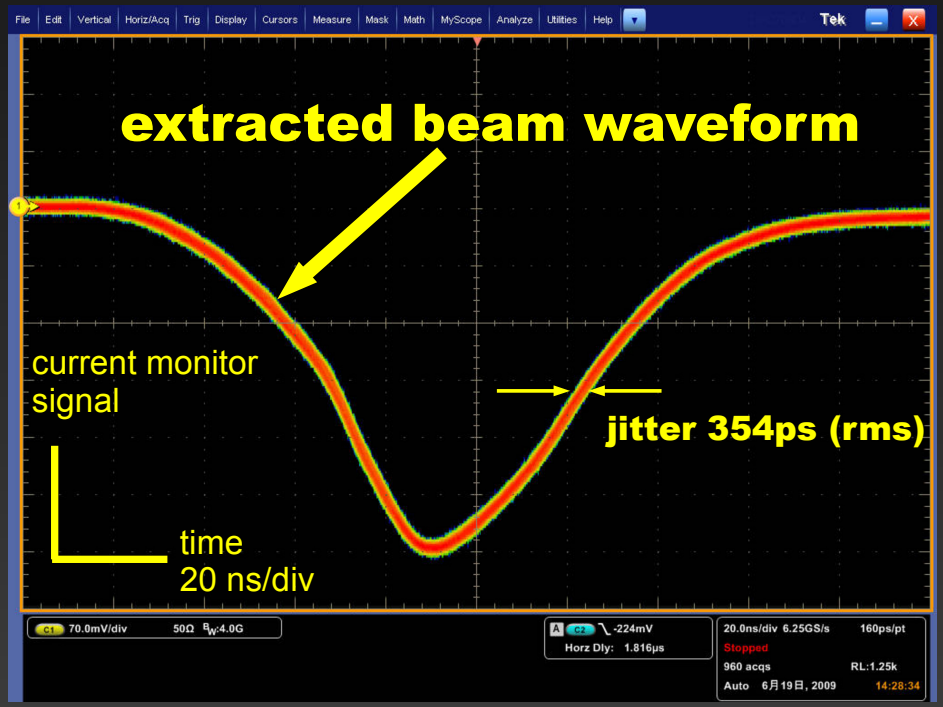

18 kW beam, superposition of $\sim$ 1000 beam waveforms at the extraction beam line. Very low timing jitter of 354 ps (RMS) was achieved.

For low intensity beams, the solution above is enough.
→ issues for high intensity beams.

Synchronization

For acceleration of high intensity beams, the phase feedback to damp the longitudinal dipole oscillation is necessary.

- phase feedback accumulates the subtle variation of the beam, and affects the extraction beam phase
- source of pulse-to-pulse jitter

Low beam jitter and suppression of oscillation, both must be achieved.

Solution:
The source of dipole oscillation is during the beginning of acceleration

- apply a gain pattern for phase feedback. The gain is maximum until the middle of acceleration, is reduced toward the end of acceleration. It becomes zero just before extraction
- at the extraction, rf / beam phase is as programmed

$\rightarrow$ minimum pulse-to-pulse jitter of 1.7 ns (full width) achieved

Synchronization

For acceleration of high intensity beams, the phase feedback to damp the longitudinal dipole oscillation is necessary.

- phase feedback accumulates the subtle variation of the beam, and affects the extraction beam phase
- source of pulse-to-pulse jitter

Low beam jitter and suppression of oscillation, both must be achieved.

Solution:
The source of dipole oscillation is during the beginning of acceleration

- apply a gain pattern for phase feedback. The gain is maximum until the middle of acceleration, is reduced toward the end of acceleration. It becomes zero just before extraction
- at the extraction, rf / beam phase is as programmed

→ minimum pulse-to-pulse jitter of 1.7 ns (full width) achieved

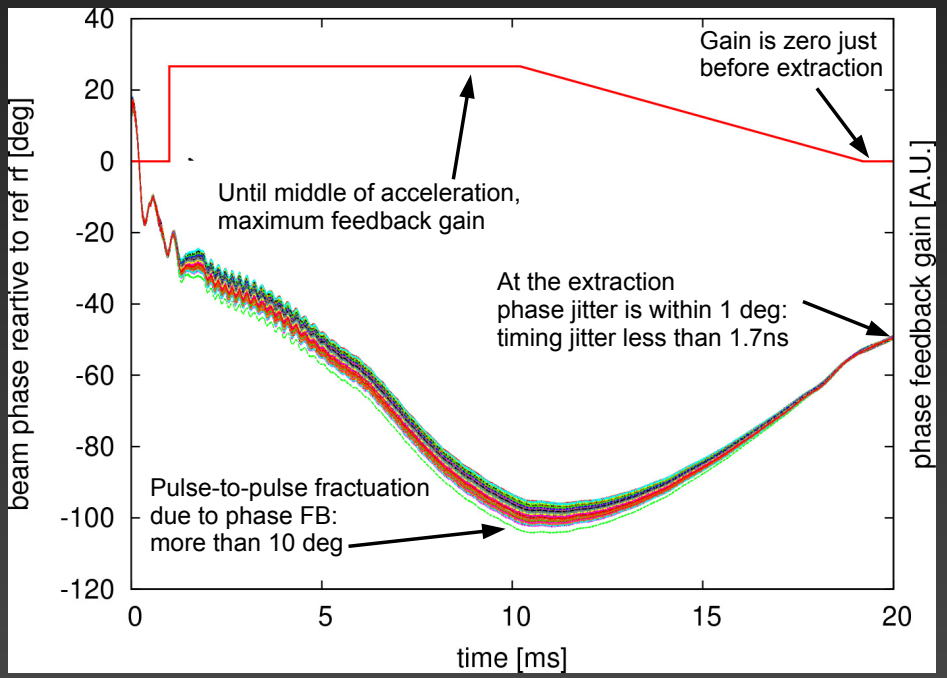

The phase feedback gain pattern and detected beam phase of 200 shots during 300 kW beams operation.

Beam loading compensation by feedforward

J-PARC RCS/MR parameters

parameter	RCS	MR
circumference	348.333 m	1567.5 m
energy	(until 2013) 0.181–3 GeV (from 2014) 0.400–3 GeV	3–30 GeV
beam intensity	(design) 8.3×10^{13} ppp (achieved) 8.3×10^{13} ppp	(achieved) 1.8×10^{14} ppp
repetition freq/period	25 Hz	2.48 s
accelerating frequency	(until 2013) 0.938–1.671 MHz (from 2014) 1.227–1.671 MHz	1.671–1.721 MHz
harmonic number	2	9
maximum rf voltage	440 kV	280 kV
No. of cavities	12	8 (+1 for 2nd)
Q-value of rf cavity	2	22

For beam loading, cavity Q value is important:

- RCS: $Q = 2$
- MR: $Q = 22$

Wake voltage in J-PARC MA cavities

RCS ($Q = 2$):

- covers wide accelerating frequency sweep (0.938–1.671 MHz) without tuning bias
- bunch shaping by second harmonic is possible
- wake contains higher harmonic components

MR ($Q = 22$):

- driven by single harmonic ($h = 9$)
- covers accelerating frequency (1.67–1.72 MHz) and neighbor harmonics ($h = 8, 10$)
- not all buckets are filled; periodic transient
- possible source of coupled bunch instability

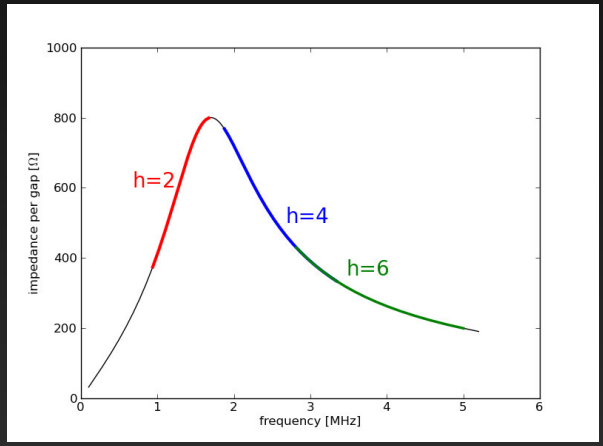

RCS cavity gap impedance ($Q = 2$).

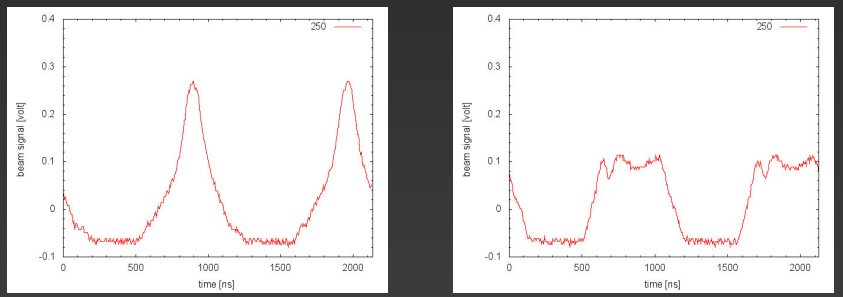

WCM waveform just after injection (left) without and (right) with dual harmonic operation.

Wake voltage in J-PARC MA cavities

RCS ($Q = 2$):

- covers wide accelerating frequency sweep (0.938–1.671 MHz) without tuning bias
- bunch shaping by second harmonic is possible
- wake contains higher harmonic components

MR ($Q = 22$):

- driven by single harmonic ($h = 9$)
- covers accelerating frequency (1.67–1.72 MHz) and neighbor harmonics ($h = 8, 10$)
- not all buckets are filled; periodic transient
- possible source of coupled bunch instability

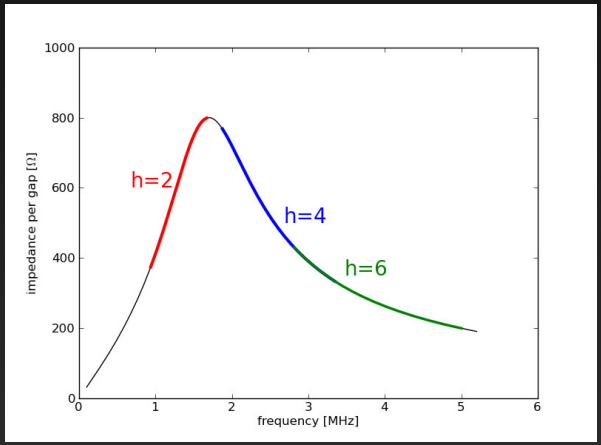

RCS cavity gap impedance ($Q = 2$).

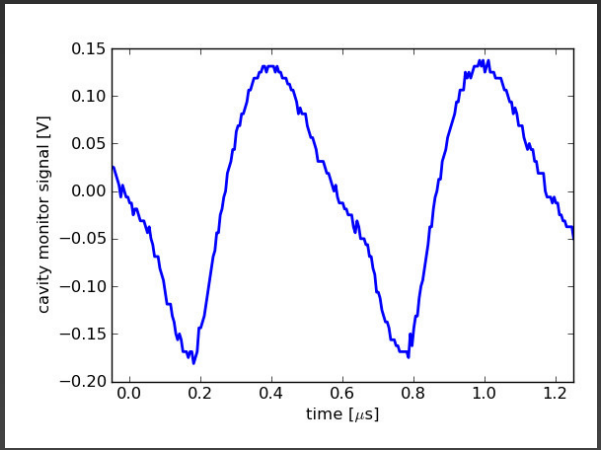

Wake voltage just before extraction (measured by turn off accelerating voltage)

Wake voltage in J-PARC MA cavities

RCS ($Q = 2$):

- covers wide accelerating frequency sweep (0.938–1.671 MHz) without tuning bias
- bunch shaping by second harmonic is possible
- wake contains higher harmonic components

MR ($Q = 22$):

- driven by single harmonic ($h = 9$)
- covers accelerating frequency (1.67–1.72 MHz) and neighbor harmonics ($h = 8, 10$)
- not all buckets are filled; periodic transient
- possible source of coupled bunch instability

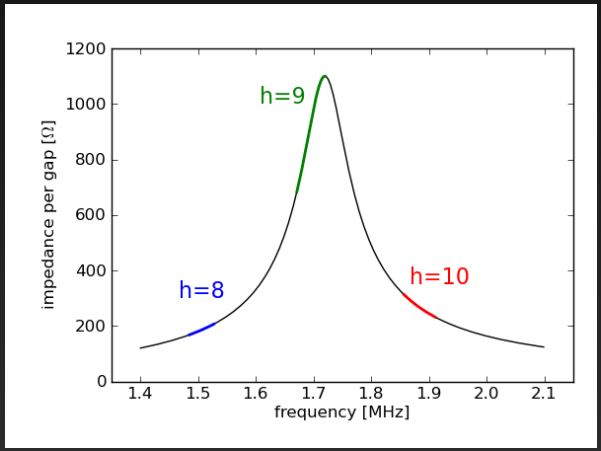

MR cavity gap impedance ($Q = 22$).

Wake voltage in J-PARC MA cavities

RCS ($Q = 2$):

- covers wide accelerating frequency sweep (0.938–1.671 MHz) without tuning bias
- bunch shaping by second harmonic is possible
- wake contains higher harmonic components

MR ($Q = 22$):

- driven by single harmonic ($h = 9$)
- covers accelerating frequency (1.67–1.72 MHz) and neighbor harmonics ($h = 8, 10$)
- not all buckets are filled; periodic transient
- possible source of coupled bunch instability

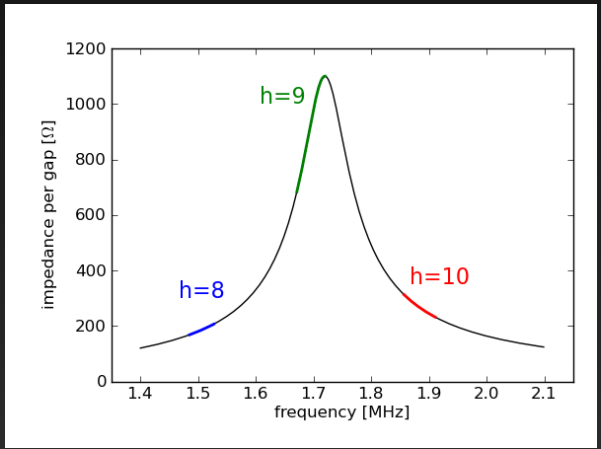

MR cavity gap impedance ($Q = 22$).

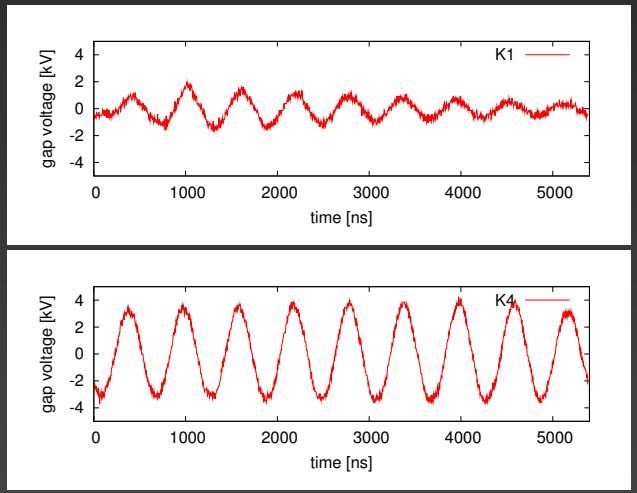

Typical waveform of the wake voltage (top) two bunches and (bottom) eight bunches are accumulated. Amplitude modulation is visible in case of two bunches.

In both RCS and MR, multiharmonic beam loading compensation is necessary.

Multiharmonic rf feedforward

J-PARC RCS and MR employ rf feedforward method for multiharmonic beam loading compensation.

- in case of direct rf feedback, FB amplifier must be located in tunnel near cavity, limited space

Feedforward method:

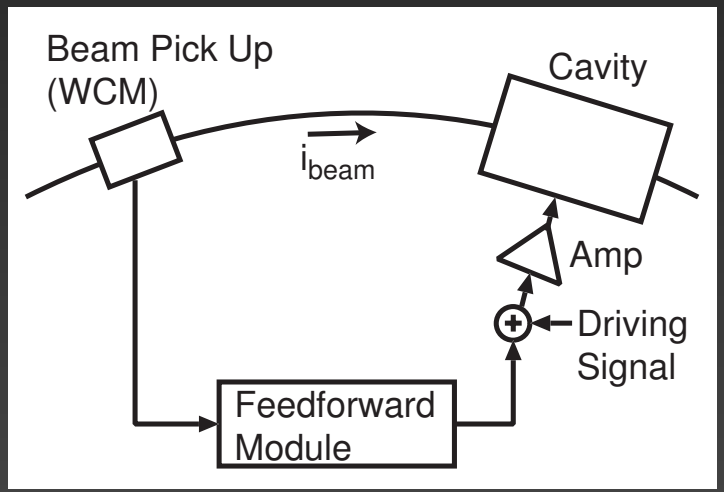

Conceptual diagram of rf feedforward method.

- pick up beam current by WCM
- in addition to driving rf current to generate accelerating voltage, $-i_{beam}$ fed to cavity
  - cancel wake voltage

Multiharmonic rf feedforward system

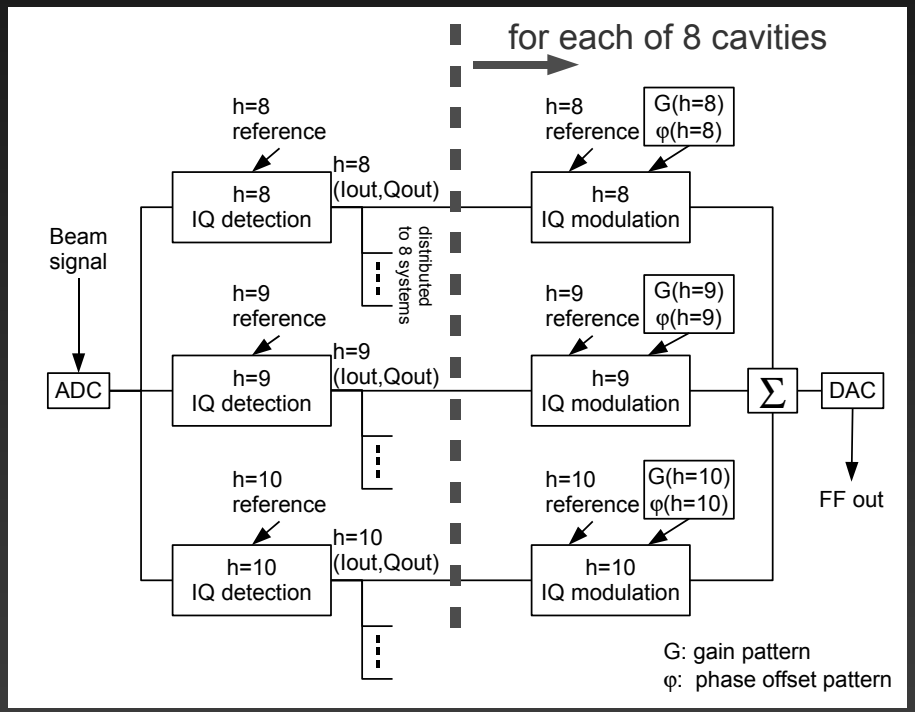

Block diagram of feedforward for MR. RCS version is similar but the selected harmonics are $h = 2, 4, 6$.

- I/Q vectors ($h = 8, 9, 10$) are generated from WCM signal
- distributed to each cavity system
- for each cavity and harmonic, gain and phase patterns are programmed. By I/Q modulation, compensation rf signal generated
- tracking BPF with passbands at ($h = 8, 9, 10$) with arbitrary gain and phase

Delicate adjustments of the gain and phase patterns are necessary. We established the commissioning methodology.

Commissioning methodology

Cavity voltage is superposition of driving rf, wake, FF component

for the selected harmonic h,

$$V_{\mathrm{cav}}(h,t) =$$
$$V_{\mathrm{cav,dr}}(h,t) + V_{\mathrm{cav,wake}}(h,t) + V_{\mathrm{cav,FF}}(h,t)$$
$$= H_{\mathrm{dr}}^{\mathrm{cav}}(h,t)\cdot V_{\mathrm{dr}}(h,t) + Z'_{\mathrm{cav}}(h,t)\cdot I_{\mathrm{beam}}(h,t)$$
$$+ Z_{\mathrm{FF}}(h,t)\cdot I_{\mathrm{beam}}(h,t)$$

(V_{cav}, V_{dr}, I_{beam}: complex amplitude)

cavity voltage is a superposition of driving rf voltage, wake, and feedforward: separation of them is important to analyze the impedance seen by the beam, however, they cannot be measured directly.
→ From V_{cav}, V_{dr}, I_{beam}, transfer functions and impedance are obtained

- waveforms from injection to extraction are taken by a long memory oscilloscope (RCS: 200 Ms/s, 4 M points)
- harmonic analysis by PC
  1. LLRF driving rf: $V_{\mathrm{dr}}(h,t)$
  2. WCM signal: $I_{\mathrm{beam}}(h,t)$
  3. cavity voltage monitor: $V_{\mathrm{cav}}(h,t)$

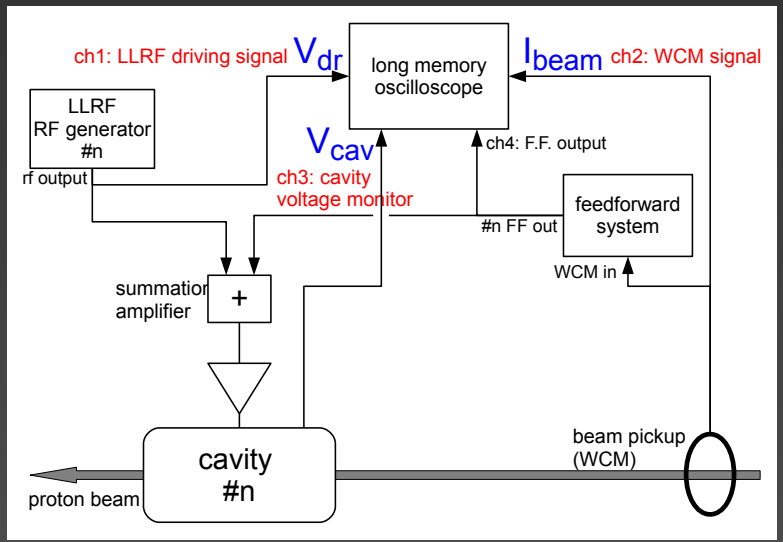

Commissioning methodology

Cavity voltage is superposition of driving rf, wake, FF component

for the selected harmonic h,

$$V_{\mathrm{cav}}(h,t) =$$
$$V_{\mathrm{cav,dr}}(h,t) + V_{\mathrm{cav,wake}}(h,t) + V_{\mathrm{cav,FF}}(h,t)$$
$$= H_{\mathrm{dr}}^{\mathrm{cav}}(h,t)\cdot V_{\mathrm{dr}}(h,t) + Z'_{\mathrm{cav}}(h,t)\cdot I_{\mathrm{beam}}(h,t)$$
$$+ Z_{\mathrm{FF}}(h,t)\cdot I_{\mathrm{beam}}(h,t)$$

(V_{cav}, V_{dr}, I_{beam}: complex amplitude)

cavity voltage is a superposition of driving rf voltage, wake, and feedforward: separation of them is important to analyze the impedance seen by the beam, however, they cannot be measured directly.
$\rightarrow$ From V_{cav}, V_{dr}, I_{beam}, transfer functions and impedance are obtained

- $H_{\mathrm{dr}}^{\mathrm{cav}}(h,t)$: transfer function from LLRF driving signal to gap voltage, obtained without accelerating beam

$$H_{\mathrm{dr}}^{\mathrm{cav}}(h,t) = \frac{V_{\mathrm{cav}}(h,t)}{V_{\mathrm{dr}}(h,t)}$$

- $Z'_{\mathrm{cav}}(h,t)$: cavity impedance under the tube current for generating the accelerating voltage, obtained without FF.

$$V_{\mathrm{cav}}(h,t) = V_{\mathrm{cav,dr}}(h,t) + V_{\mathrm{cav,wake}}(h,t)$$
$$= H_{\mathrm{dr}}^{\mathrm{cav}}(h,t)\cdot V_{\mathrm{dr}}(h,t) + Z'_{\mathrm{cav}}(h,t)\cdot I_{\mathrm{beam}}(h,t)$$

Commissioning methodology

Cavity voltage is superposition of driving rf, wake, FF component

for the selected harmonic h,

$V_{\mathrm{cav}}(h,t) =$

$V_{\mathrm{cav,dr}}(h,t) + V_{\mathrm{cav,wake}}(h,t) + V_{\mathrm{cav,FF}}(h,t)$

$= H_{\mathrm{dr}}^{\mathrm{cav}}(h,t) \cdot V_{\mathrm{dr}}(h,t) + Z'_{\mathrm{cav}}(h,t) \cdot I_{\mathrm{beam}}(h,t)$

$+ Z_{\mathrm{FF}}(h,t) \cdot I_{\mathrm{beam}}(h,t)$

(V_{cav}, V_{dr}, I_{beam}: complex amplitude)

cavity voltage is a superposition of driving rf voltage, wake, and feedforward: separation of them is important to analyze the impedance seen by the beam, however, they cannot be measured directly.
$\rightarrow$ From V_{cav}, V_{dr}, I_{beam}, transfer functions and impedance are obtained

- $Z_{\mathrm{FF}}(h,t)$: transfer function from beam current to FF component (obtained with FF.)
- impedance seen by the beam with FF: $Z'_{\mathrm{cav}}(h,t) + Z_{\mathrm{FF}}(h,t)$
  To minimize the impedance, pattern is modified

$$|Z_{\mathrm{FF}}(h,t)| = |Z'_{\mathrm{cav}}(h,t)|$$

$$\mathrm{Arg}(Z_{\mathrm{FF}}(h,t)) = -\mathrm{Arg}(Z'_{\mathrm{cav}}(h,t))$$

- by several iterations, impedance seen by the beam can be greatly reduced

Commissioning methodology of feedforward has been established.

RCS commissioning results

Commissioned using 300 kW eq. (2.5×10^{13} ppp) high intensity beams.

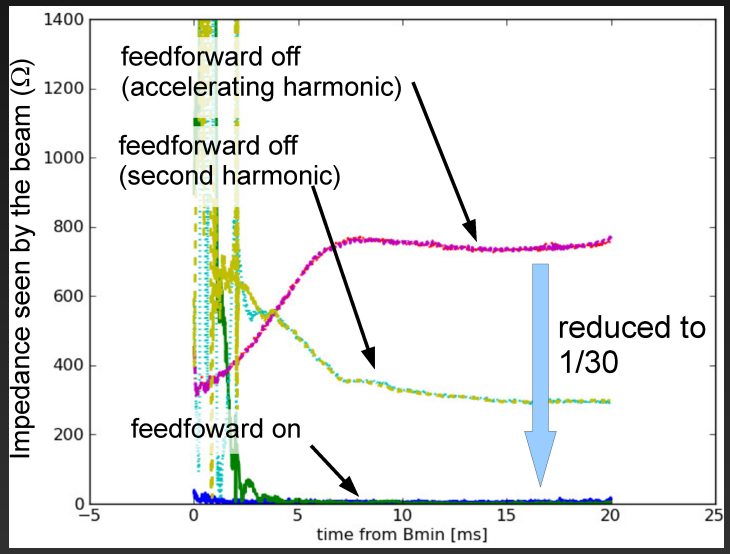

Comparison of impedance seen by the beam without and with feedforward.

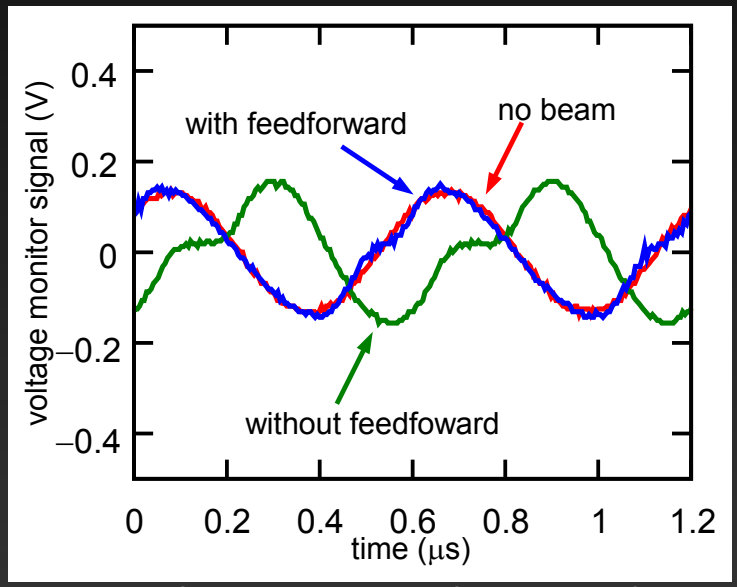

Comparison of gap voltage waveform just before extraction.

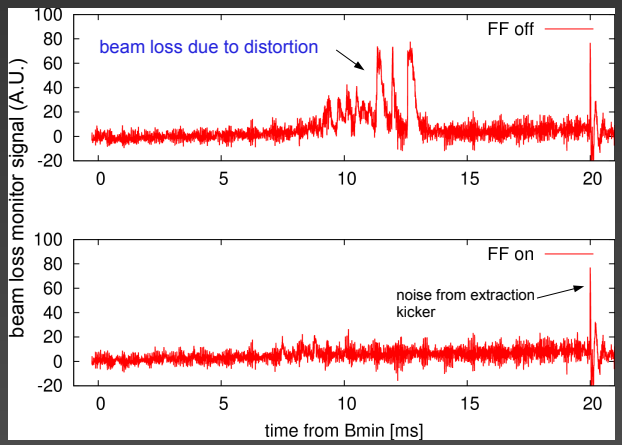

BLM signal at the arc section.

- impedance seen by the beam is successfully suppressed (1/30)
- distortion reduced, waveform with FF is close to the case of no beam
- phase delay, which corresponds to the loading angle, is reduced
- beam loss due to the distortion disappeared

MR commissioning results

Commissioned using 200 kW eq. (1.0×10^{14} ppp) high intensity beams. Impedance seen by the beam for ($h = 8, 9, 10$) successfully reduced.

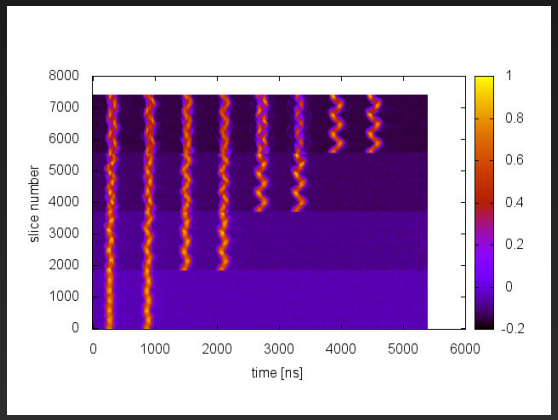

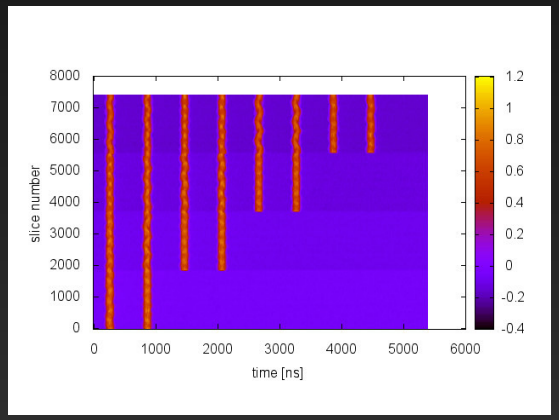

Mountain plots of WCM during injection period without FF.

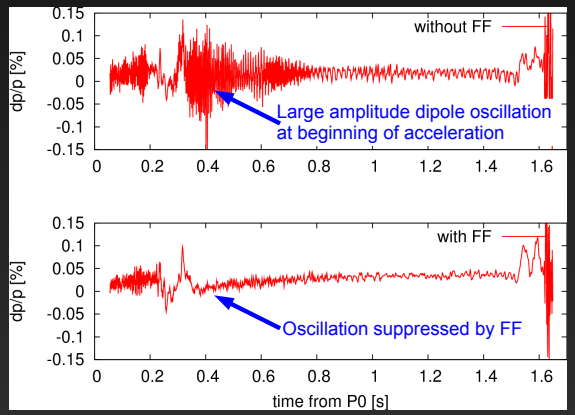

dp/p from injection to extraction Without FF (top) and with FF (bottom).

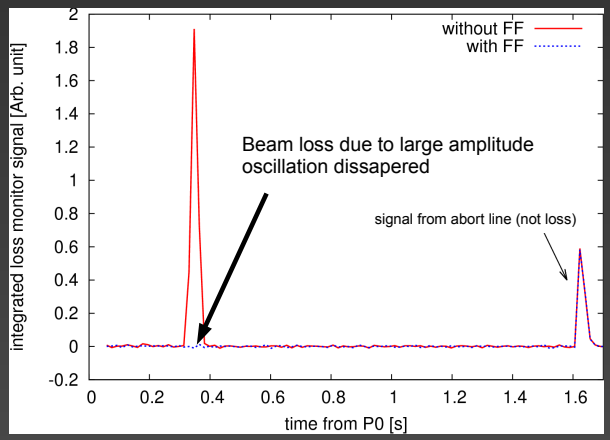

Typical beam loss monitor signal in the arc sections without and with feedforward.

- by FF, rf phase jumps due to loading angle are reduced, less dipole oscillation
- compensation of neighbor harmonics ($h = 8, 10$): periodic transient reduced, forward and rear bunches oscillate similarly
- oscillation reduced throughout the accelerating period
- beam losses in the arc sections due to large amplitude dipole oscillation disappeared

J-PARC FF system summary

- multiharmonic feedforward system developed for RCS and MR
- commissioning methodology established
- feedforward compensation is now indispensable for high beam power operation
  - FF systems for $h = 2, 4, 6$ and $h = 1, 3, 5$ are working in RCS
  - $h = 8, 9, 10$ and $h = 17, 18, 19$, fundamental / second harmonic and neighbors in MR

Experience of 1 MW-eq beam acceleration

1 MW beam acceleration: first trial

Circulating beam intensity over the 20 ms from injection to extraction measured by CT

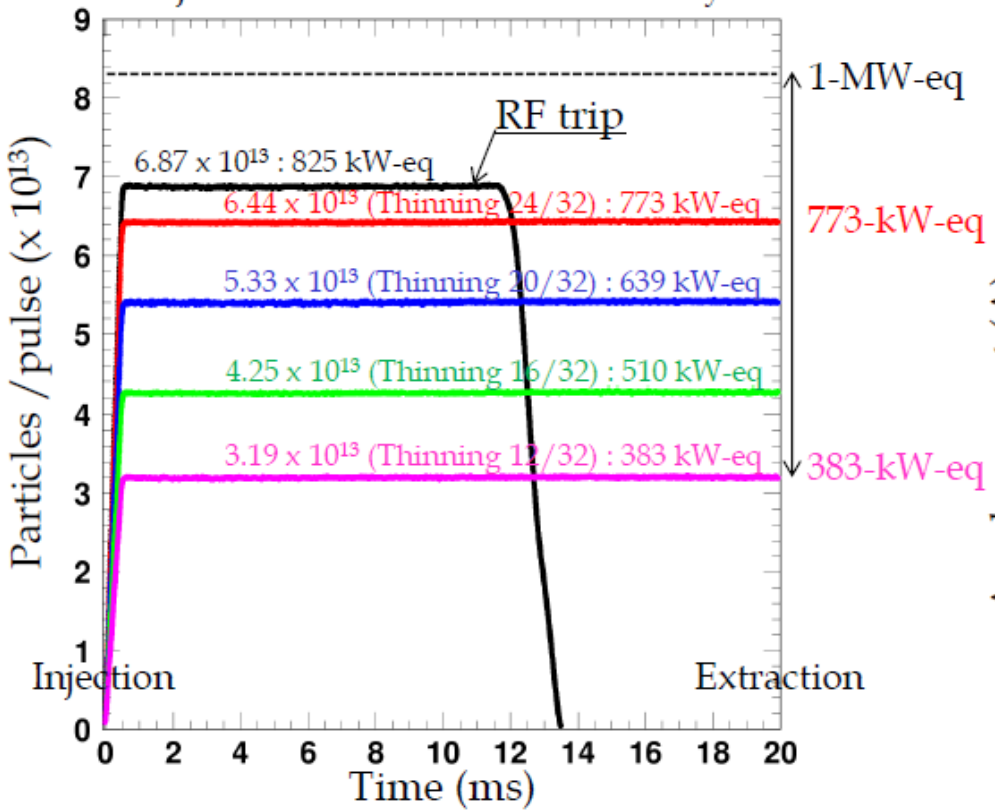

Anode current measured as a function of the beam power

W/ multi-harmonics (h=2,4,6) feed-forward for beam loading compensation

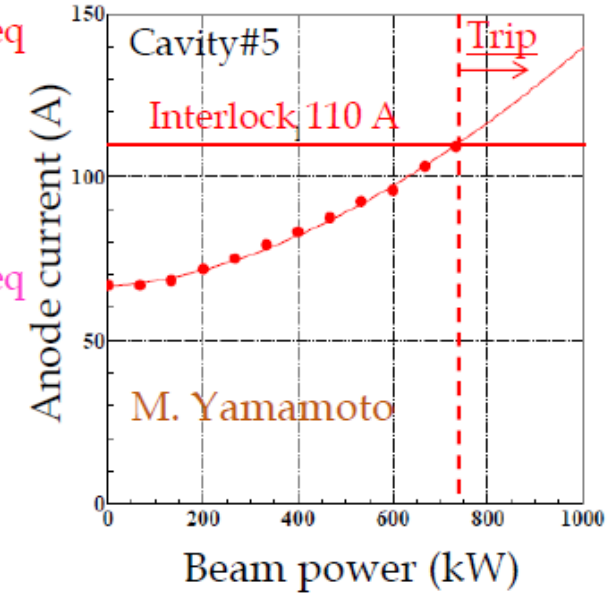

- ✓ The beam accelerations of up to 770 kW was achieved with no significant beam loss.
- ✓ But, the 1-MW beam acceleration was not reached due to the RF trip.
- ✓ When the beam intensity got to over 800 kW, the anode power supply of the RF system tripped due to the over current.

The first trial in October 2014 was not successful due to shortage of the capacity of anode power supply.

1 MW beam acceleration: quick measures

- Quick measures against the RF trip
  - ✓ The interlock level was increased;
    110 A ⇒ 125 A
  - ✓ The resonant frequency of the RF cavity was shifted to decrease the anode current required for the 1-MW beam acceleration;
    1.7 MHz ⇒ 2.1 MHz

- Date : Dec 26-27, 2014 (Run#59)
- Injection beam condition
  Injection energy : 400 MeV
  Peak current : 44.4 mA @ the entrance of RCS
  Pulse length : 0.5 ms
  Chopper beam-on duty factor : 60%
  ⇒ 8.32 x 10^{13} particles/pulse, corresponding to **999 kW** at 3 GeV

Anode current vs. Beam power

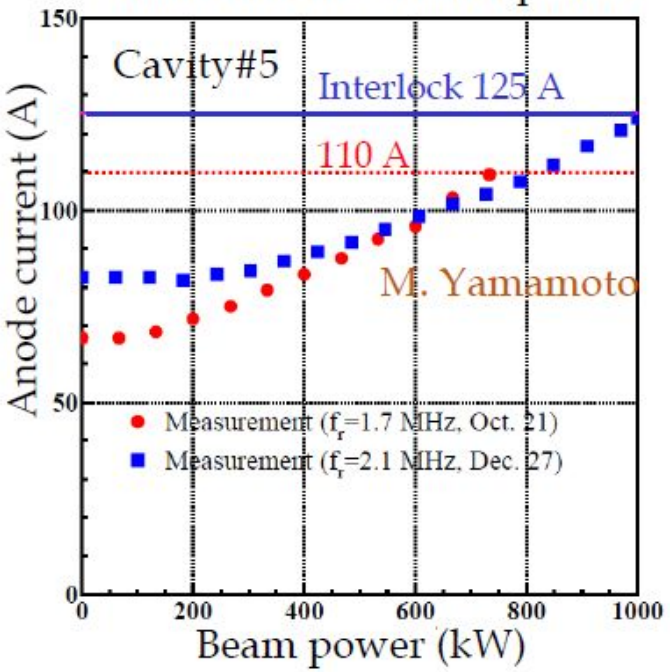

Circulating beam intensity

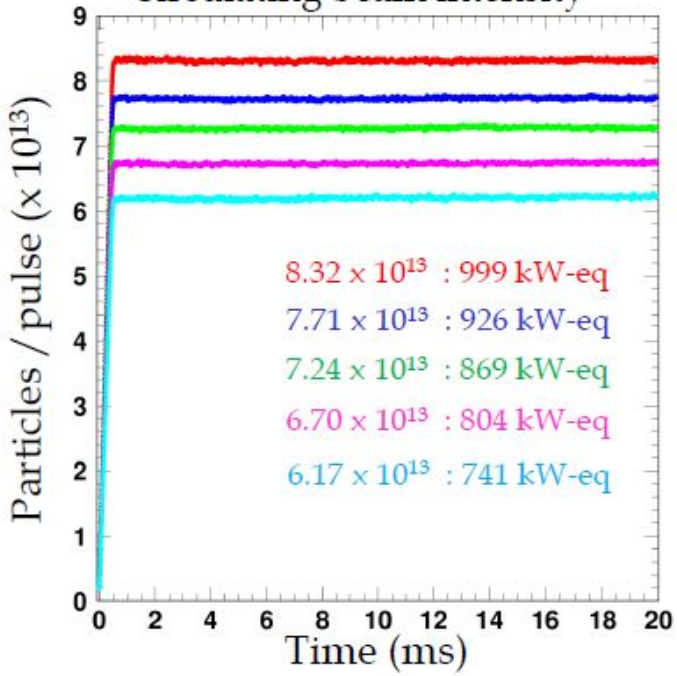

By shifting the cavity resonant frequency (1.7 → 2.1 MHz), anode currents decreased and we could accelerate 1 MW-eq beams.

1 MW beam acceleration: result of trial in Jan 2015

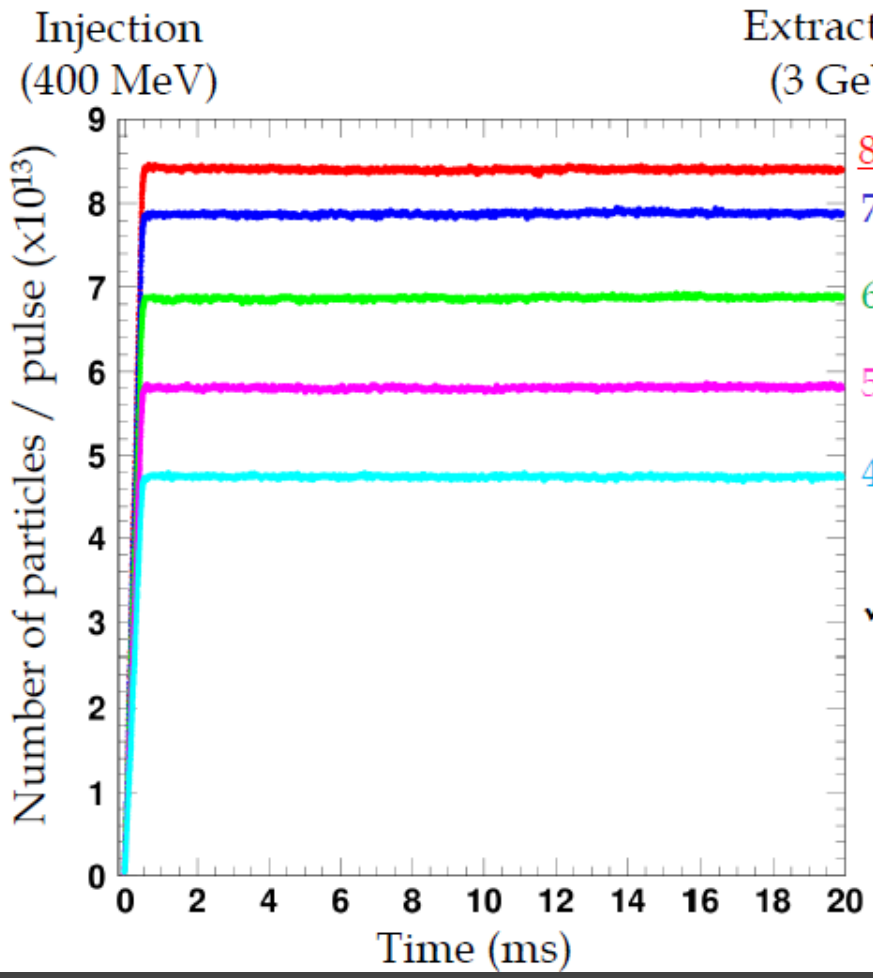

8.41 x 10^{13} (Thinning 32/32): 1010 kW-eq.

7.86 x 10^{13} (Thinning 30/32): 944 kW-eq.

6.87 x 10^{13} (Thinning 26/32): 825 kW-eq.

5.80 x 10^{13} (Thinning 22/32): 696 kW-eq.

4.73 x 10^{13} (Thinning 18/32): 568 kW-eq.

✓ The 1-MW beam acceleration was achieved !
(05:55 am, Jan. 10, 2015)

After fine tuning, no intensity loss was observed by DCCT, however...

Beam loss 1 MW beam acceleration

BLM signals @ collimator & arc sections (Scintillation type BLM)

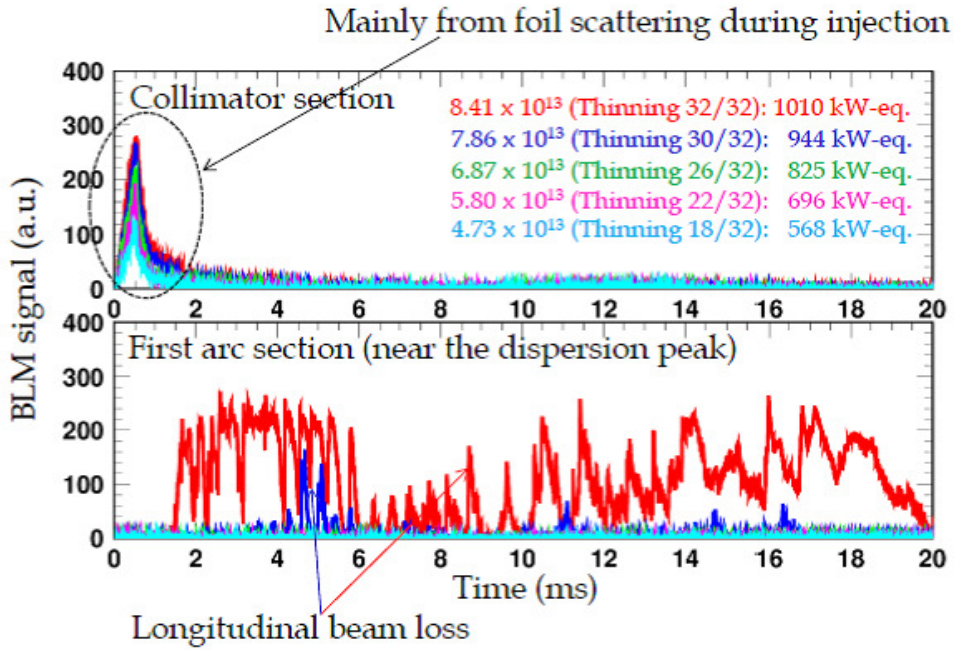

✓ RF operation in Run#60 ;
- the RF FF for h=4,6 was turned off for the Cavity#4 and Cavity#6
- the RF voltage was slightly decreased for a part of cavities to avoid the trip.

Subtle beam losses at arc sections were observed.

RF group (especially I) was not completely happy because the loss is longitudinal losses.

Beam loss 1 MW beam acceleration

BLM signals @ collimator & arc sections (Scintillation type BLM)

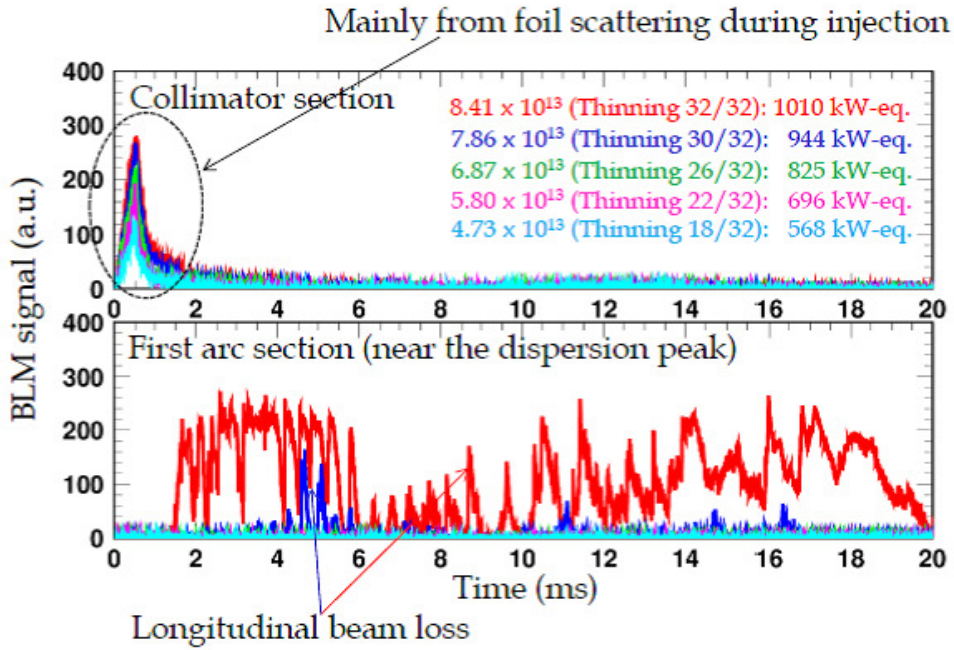

- ✓ RF operation in Run#60 ;
  - the RF FF for h=4,6 was turned off for the Cavity#4 and Cavity#6
  - the RF voltage was slightly decreased for a part of cavities to avoid the trip.

Subtle beam losses at arc sections were observed.
RF group (especially I) was not completely happy because the loss is longitudinal losses.

Comparison between 1 MW and 560 kW beams

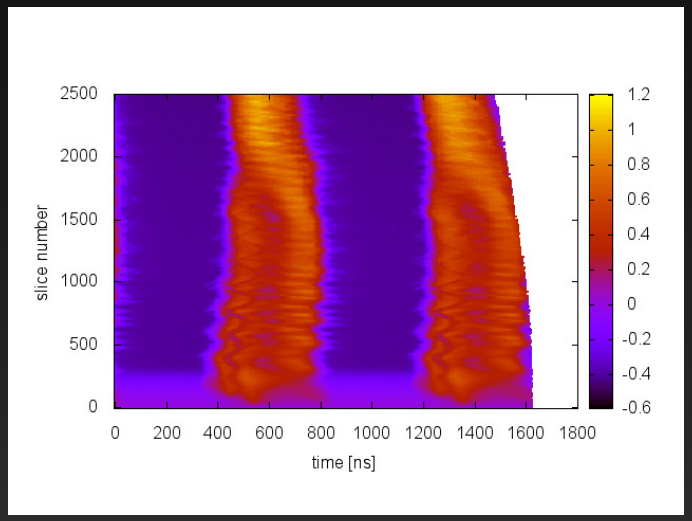

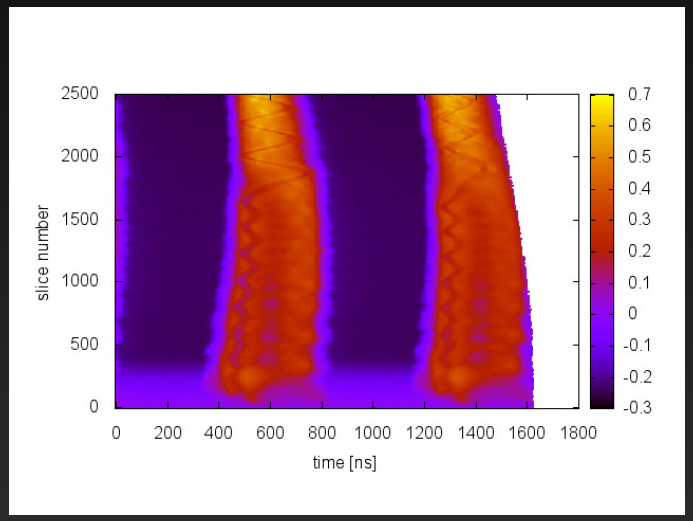

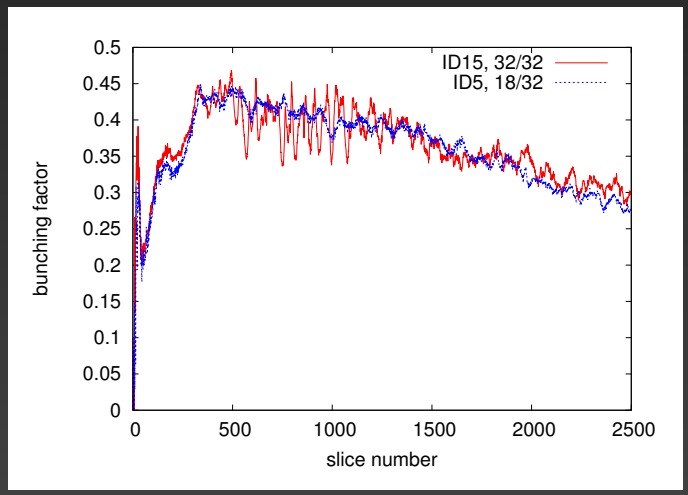

Mountain plots of 1 MW (left) and 560 kW (right) beam and comparison of bunching factor (bottom).

- Not very different
- A bit more oscillation in case of 1 MW, also B_f oscillates
- oscillation source?

Effect of wake voltage odd harmonics

After shifting of resonant frequency, sometimes front and rear bunches oscillate differently.

- beam signal and cavity voltage have odd harmonics components

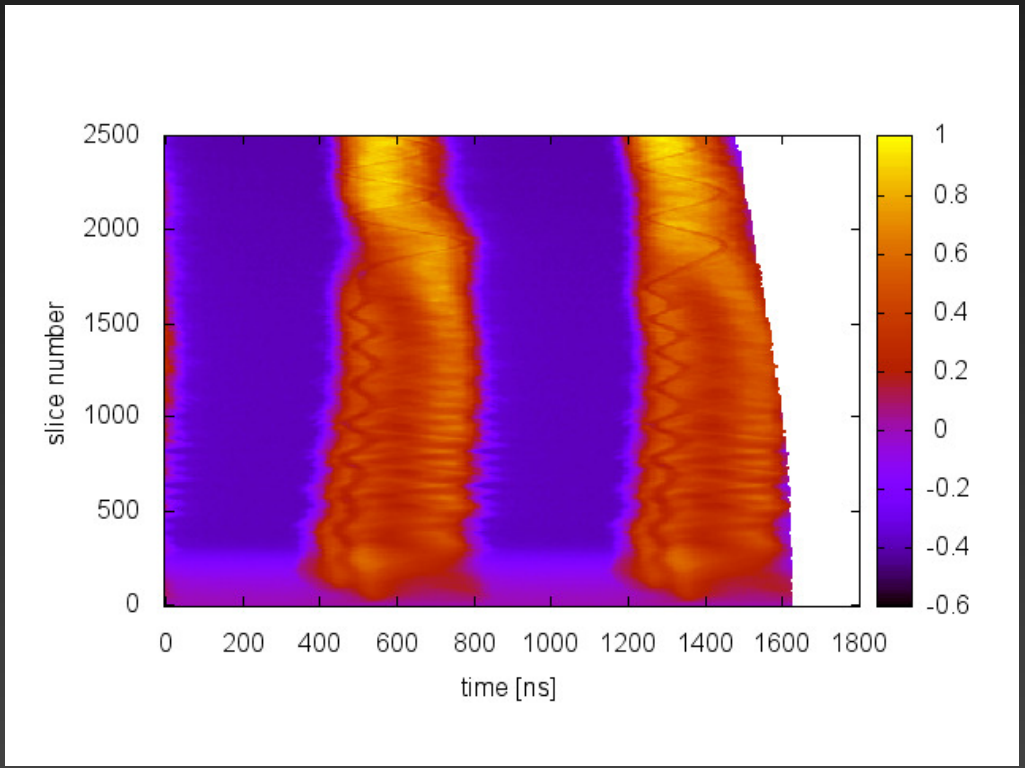

Effect of wake voltage odd harmonics

After shifting of resonant frequency, sometimes front and rear bunches oscillate differently.

- beam signal and cavity voltage have odd harmonics components

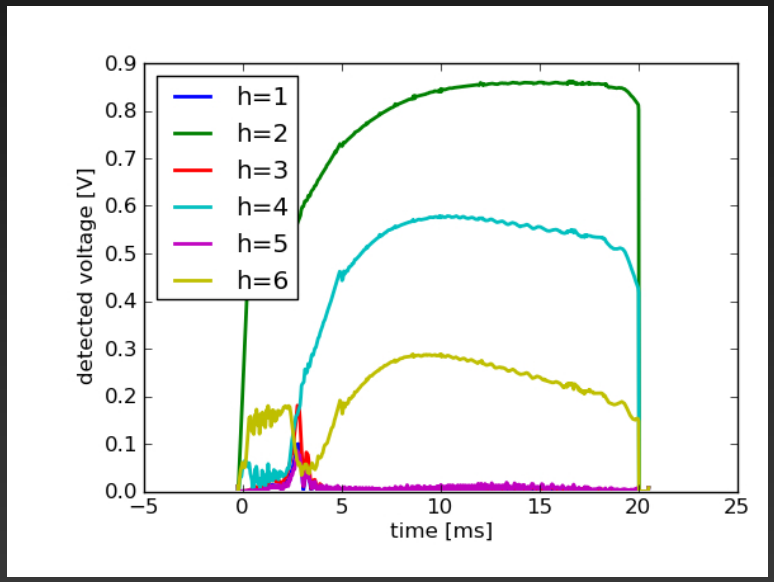

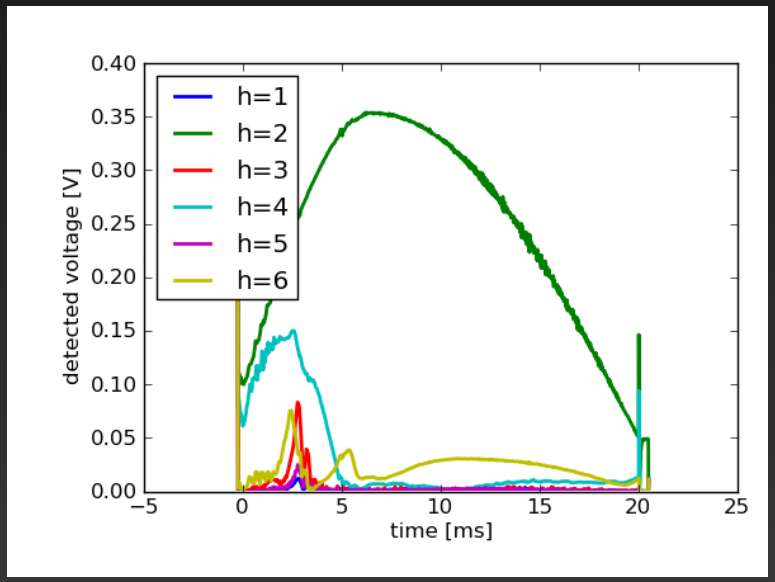

Harmonic components of (left) beam signal and (right) cavity voltage monitor. Odd harmonics are significant around 2–3 ms.

The resonant frequency shift is good for reduction of anode current, but not best for longitudinal motion.

- feedforward of odd harmonics is not sufficient to suppress this kind of wake
- narrow band voltage feedback is now considered in addition to feedforward

Conclusion

- LLRF control systems for J-PARC RCS and MR were designed and built to handle multiharmonic rf signals,
  - voltage control
  - phase feedback

  and the systems work properly
- multiharmonic beam loading compensation by rf feedforward greatly reduces impedance seen by the beam
- improvements foreseen toward our goal
  - anode power supply consolidation is planned this summar
  - narrowband vector voltage control is considered

Backup slides

Dual harmonic AVC

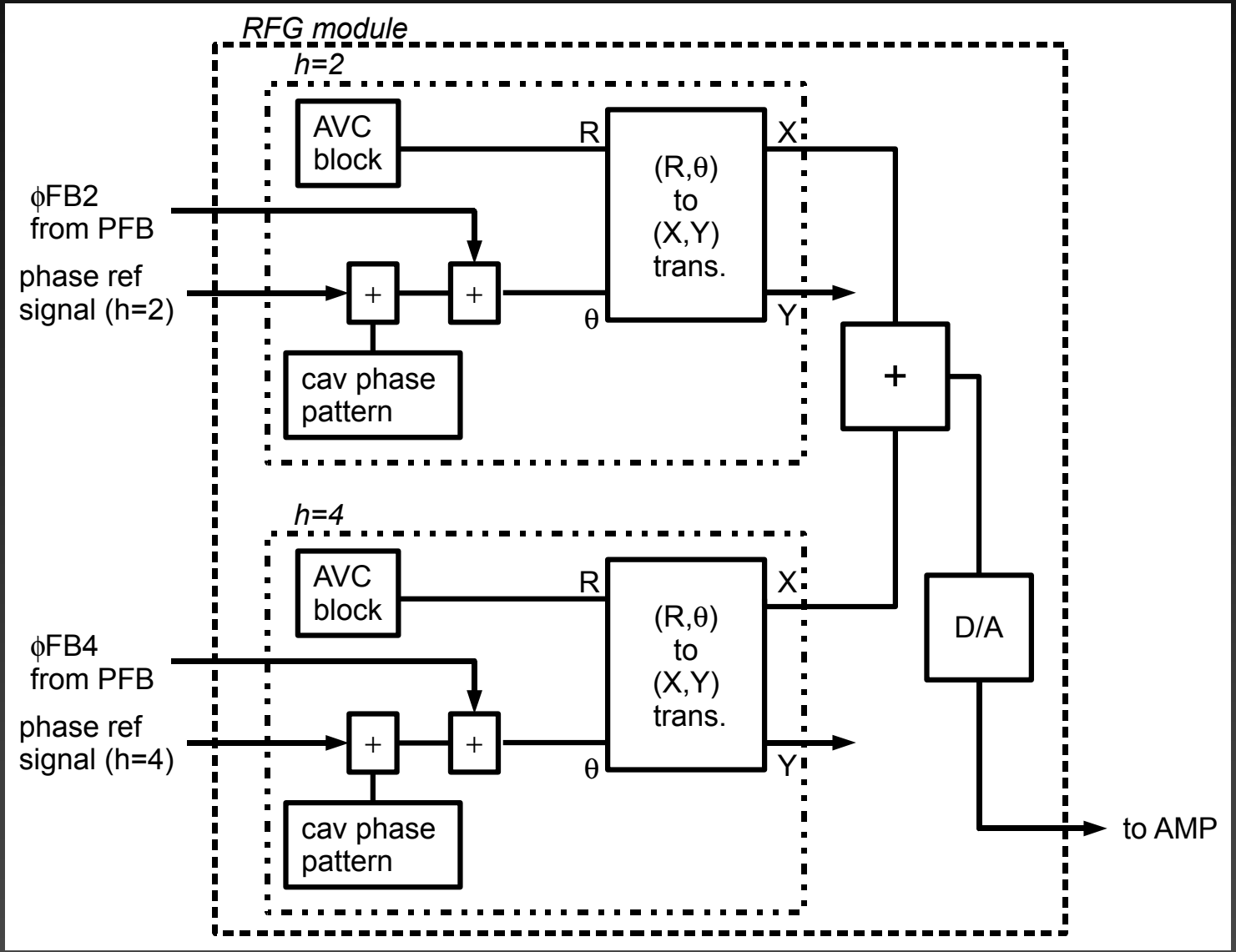

Phase feedback

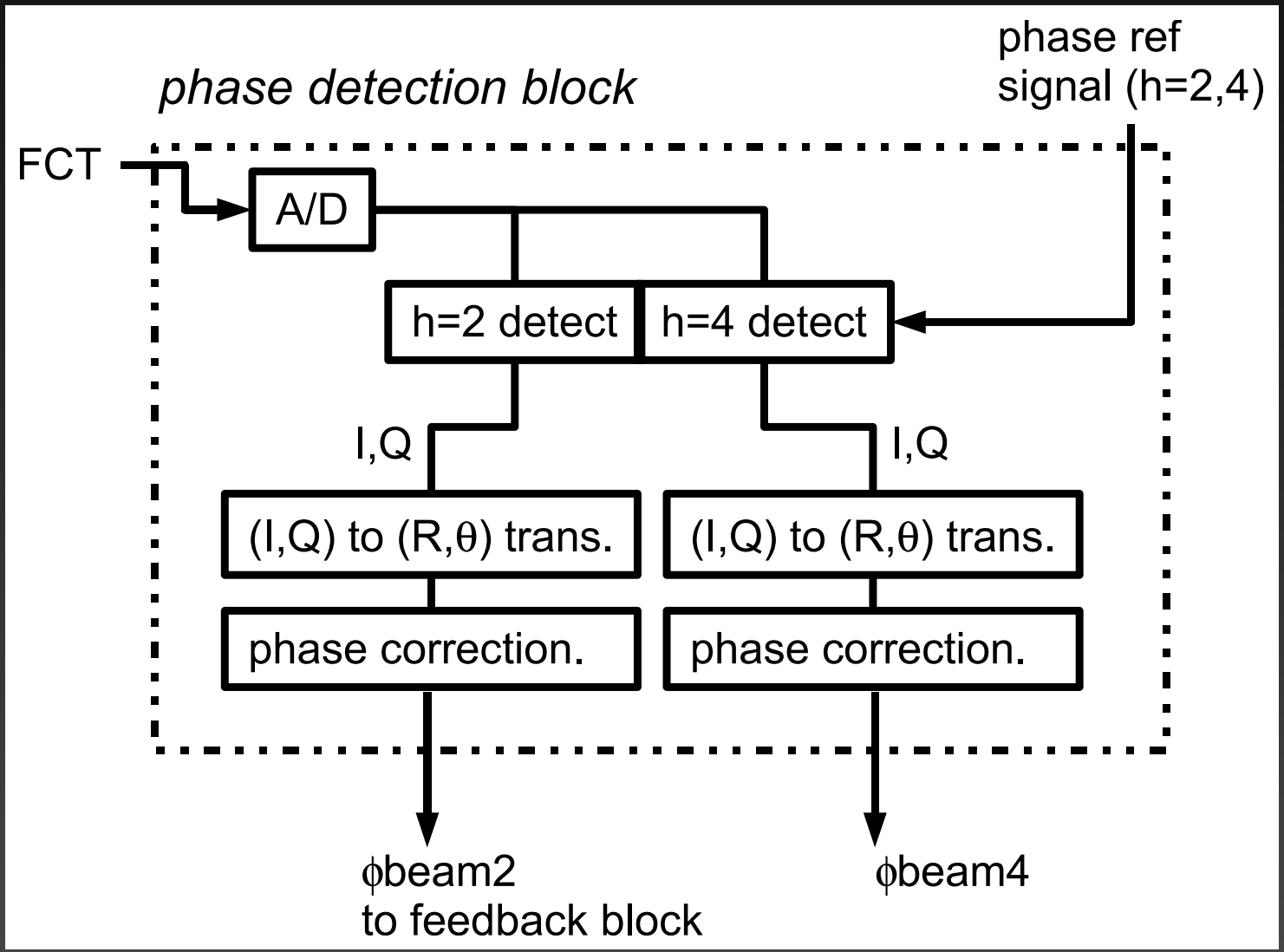

Vector sum

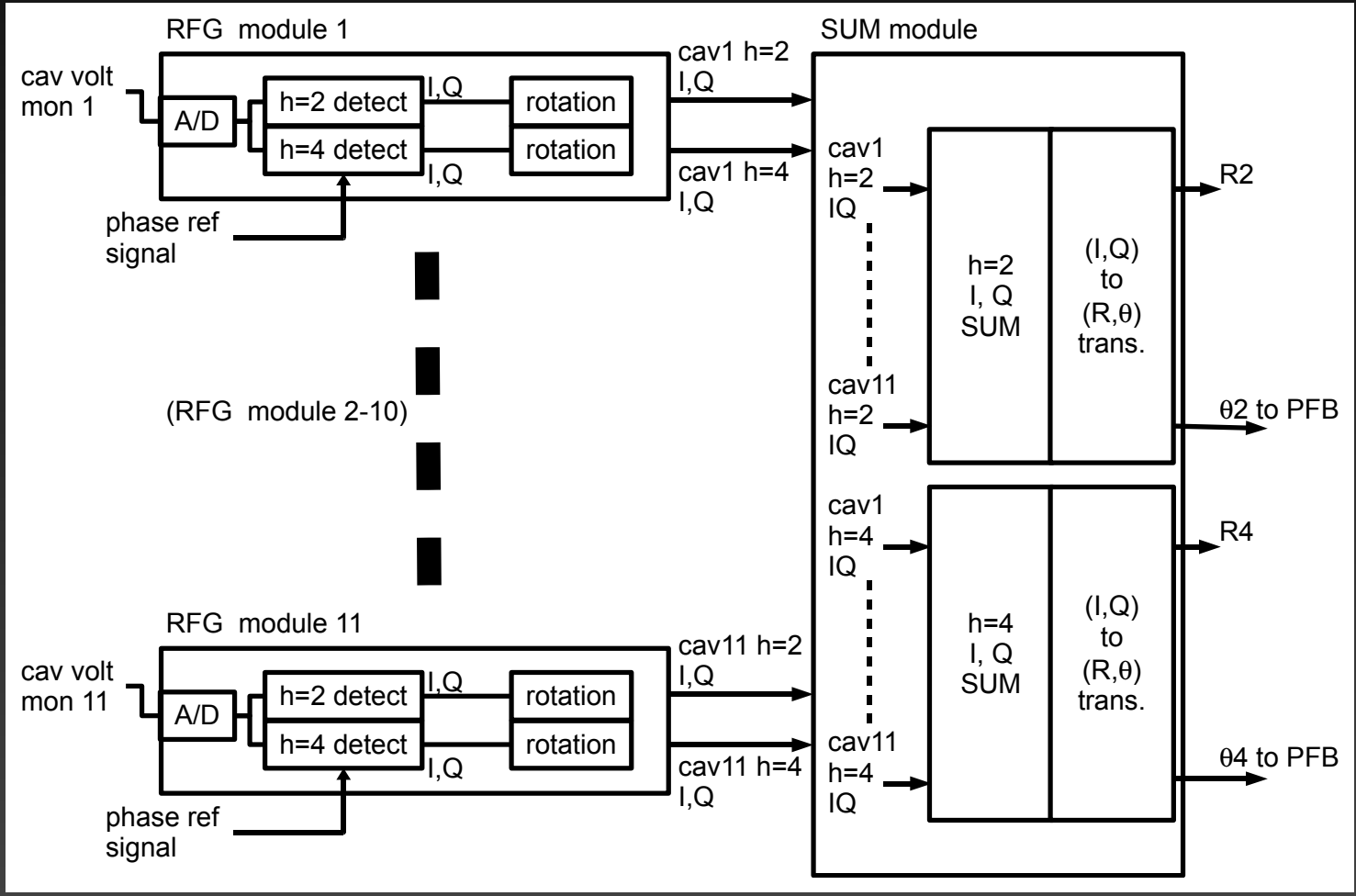

Vector sum of cavity voltage for phase detection.

Phase feedback